



NASA's Evolutionary Xenon Thruster (NEXT) Prototype Model 1R (PM1R) Ion Thruster and Propellant Management System Wear Test Results

*Jonathan L. Van Noord and George C. Soulas
Glenn Research Center, Cleveland, Ohio*

*James S. Sovey
Alphaport, Inc., Cleveland, Ohio*

NASA STI Program . . . in Profile

Since its founding, NASA has been dedicated to the advancement of aeronautics and space science. The NASA Scientific and Technical Information (STI) program plays a key part in helping NASA maintain this important role.

The NASA STI Program operates under the auspices of the Agency Chief Information Officer. It collects, organizes, provides for archiving, and disseminates NASA's STI. The NASA STI program provides access to the NASA Aeronautics and Space Database and its public interface, the NASA Technical Reports Server, thus providing one of the largest collections of aeronautical and space science STI in the world. Results are published in both non-NASA channels and by NASA in the NASA STI Report Series, which includes the following report types:

- **TECHNICAL PUBLICATION.** Reports of completed research or a major significant phase of research that present the results of NASA programs and include extensive data or theoretical analysis. Includes compilations of significant scientific and technical data and information deemed to be of continuing reference value. NASA counterpart of peer-reviewed formal professional papers but has less stringent limitations on manuscript length and extent of graphic presentations.
- **TECHNICAL MEMORANDUM.** Scientific and technical findings that are preliminary or of specialized interest, e.g., quick release reports, working papers, and bibliographies that contain minimal annotation. Does not contain extensive analysis.
- **CONTRACTOR REPORT.** Scientific and technical findings by NASA-sponsored contractors and grantees.

- **CONFERENCE PUBLICATION.** Collected papers from scientific and technical conferences, symposia, seminars, or other meetings sponsored or cosponsored by NASA.
- **SPECIAL PUBLICATION.** Scientific, technical, or historical information from NASA programs, projects, and missions, often concerned with subjects having substantial public interest.
- **TECHNICAL TRANSLATION.** English-language translations of foreign scientific and technical material pertinent to NASA's mission.

Specialized services also include creating custom thesauri, building customized databases, organizing and publishing research results.

For more information about the NASA STI program, see the following:

- Access the NASA STI program home page at <http://www.sti.nasa.gov>
- E-mail your question via the Internet to help@sti.nasa.gov
- Fax your question to the NASA STI Help Desk at 443-757-5803
- Telephone the NASA STI Help Desk at 443-757-5802
- Write to:
NASA Center for AeroSpace Information (CASI)
7115 Standard Drive
Hanover, MD 21076-1320



NASA's Evolutionary Xenon Thruster (NEXT) Prototype Model 1R (PM1R) Ion Thruster and Propellant Management System Wear Test Results

*Jonathan L. Van Noord and George C. Soulas
Glenn Research Center, Cleveland, Ohio*

*James S. Sovey
Alphaport, Inc., Cleveland, Ohio*

Prepared for the
31st International Electric Propulsion Conference (IEPC 2009)
cosponsored by Aerojet, A.F. Office of Scientific Research, AFRL, Busek Company, Inc.,
CU Aerospace, ERPS, EDA, Inc., L3 Communications, Michigan Space Grant Consortium/NASA,
and Michigan Engineering
Ann Arbor, Michigan, September 20-24, 2009

National Aeronautics and
Space Administration

Glenn Research Center
Cleveland, Ohio 44135

Trade names and trademarks are used in this report for identification only. Their usage does not constitute an official endorsement, either expressed or implied, by the National Aeronautics and Space Administration.

Level of Review: This material has been technically reviewed by technical management.

Available from

NASA Center for Aerospace Information
7115 Standard Drive
Hanover, MD 21076-1320

National Technical Information Service
5301 Shawnee Road
Alexandria, VA 22312

Available electronically at <http://gltrs.grc.nasa.gov>

NASA's Evolutionary Xenon Thruster (NEXT) Prototype Model 1R (PM1R) Ion Thruster and Propellant Management System Wear Test Results

Jonathan L. Van Noord and George C. Soulas
National Aeronautics and Space Administration
Glenn Research Center
Cleveland, Ohio 44135

James S. Sovey
Alphaport, Inc.
Cleveland, Ohio 44135

Abstract

The results of the NEXT wear test are presented. This test was conducted with a 36-cm ion engine (designated PM1R) and an engineering model propellant management system. The thruster operated with beam extraction for a total of 1680 hr and processed 30.5 kg of xenon during the wear test, which included performance testing and some operation with an engineering model power processing unit. A total of 1312 hr was accumulated at full power, 277 hr at low power, and the remainder was at intermediate throttle levels. Overall ion engine performance, which includes thrust, thruster input power, specific impulse, and thrust efficiency, was steady with no indications of performance degradation. The propellant management system performed without incident during the wear test. The ion engine and propellant management system were also inspected following the test with no indication of anomalous hardware degradation from operation.

Nomenclature

DACS	Data Acquisition and Control System
DCA	Discharge Cathode Assembly
DCIU	Digital Control Interface Unit
EM	Engineering Model
FCD	Flow Control Device
GRC	NASA Glenn Research Center
HPA	High Pressure Assembly
JPL	NASA Jet Propulsion Laboratory
LDT	Long Duration Test
LPA	Low Pressure Assembly
NCA	Neutralizer Cathode Assembly
NEXT	NASA's Evolutionary Xenon Thruster
NSTAR	NASA Solar Electric Propulsion Technology Application Readiness
PFCV	Proportional Flow Control Valve
PM	Prototype Model
PMS	Propellant Management System
PPU	Power Processing Unit
TRL	Technology Readiness Level
VF5	Vacuum Facility 5
XFSE	Xenon Feed System Equipment

Introduction

NASA's Evolutionary Xenon Thruster (NEXT) project includes the development of a high performance, nominal 7-kW, Electric Propulsion Thruster; a light weight, high efficiency power processing unit (PPU); a highly flexible advanced Propellant Management System (PMS); and a light-weight, low-cost gimbal (Refs. 1 and 2). The goal of the NEXT project is to develop the next generation ion propulsion technology to NASA Technology Readiness Level (TRL) 6 (Ref. 3). The NEXT project has built on knowledge gained from the current state-of-the-art NASA Solar Electric Propulsion Technology Application Readiness (NSTAR) thruster system to create a more efficient, higher specific impulse, and lower specific mass system (Ref. 2). The design approach will provide future NASA science missions with the greatest value in mission performance at a low total development cost.

Several potential missions have been evaluated using the NEXT system (Ref. 4). These missions included a Saturn mission, Neptune mission, a near Earth asteroid return, comet rendezvous, Vesta-Ceres rendezvous, Titan direct lander, and a comet surface sample return. A 300 kg xenon throughput requirement, which is a total impulse of 1.23×10^7 N-s at full power, was derived from these studies with a corresponding 450 kg qualification level (Ref. 1).

Previous extended testing by the NSTAR program examined the wear mechanisms for ion thrusters (Refs. 5, 6, 7, and 8). Several of these wear mechanisms were minimized and mitigated during the NSTAR program, but a set of life-limiting mechanisms was established. A review of previous ion thruster endurance tests along with the causes of failure is given in Reference 9. Based on these related failure modes, an initial life assessment of the NEXT thruster was prepared during Phase I of the NEXT program (Ref. 10). To date several iterations of life models have been utilized based on the most recent data available for the NEXT thruster. These have included deterministic models for the ion optics (Refs. 11, 12, and 13), and the hollow cathodes (Refs. 10 and 14). The most recent life assessments for the NEXT ion thruster are given in Reference 15 and 16. Further work is continuing to reduce uncertainties involved in the life assessment, such as measurement of the grid gap during extended operation (Refs. 17 and 18).

Several extended duration tests of the NEXT thruster and its components to evaluate wear mechanisms have already been completed. The NEXT Engineering Model 1 (EM1) thruster was wear-tested for 2038 hr (43 kg of xenon throughput) to evaluate thruster wear (Ref. 19). Two wear mechanisms were revealed that could potentially lead to a premature failure. One was the excessive wear on the discharge cathode keeper orifice plate and the other was excessive wear on the accelerator grid outer radius holes. While loss of the keeper orifice plate does not result in thruster failure, the keeper electrode does protect the cathode and extend its life. The keeper material was changed to graphite for subsequent designs to achieve significant margin for life. The ion optics design was modified by removing some of the outer holes and making the effective beam diameter 36 cm instead of the previous 40 cm. The removal of holes was only in regions of low plasma density resulting in similar discharge losses without the added optics wear.

The NEXT Engineering Model 3 (EM3) is currently undergoing a Long Duration Test (LDT) at the NASA Glenn Research Center (GRC) (Refs. 17, 18, and 20). The objectives of this test is to validate and qualify the NEXT propellant throughput capability to a qualification-level of 450 kg. EM3 has processed 434 kg of xenon and operated for 24,400 hr (Refs. 20 and 21). Thruster operation to date has been at a beam power supply voltage of 1800 V and a beam current of 3.52 A for the first ~13,000 hr, followed by a lower voltage of 1179 V at the same beam current for 6500 hr, and subsequently throttled to low power throttle points. While the EM3 thruster was designed and built at GRC, the EM3 thruster optics assembly was built by the same manufacturer and to the same specifications as the Prototype Model (PM) thruster. Modeling and the LDT show that the initial failure mechanism is from pit and groove erosion on the ion optics accelerator grid after 750 kg of xenon throughput (Refs. 15 and 20).

The design of the GRC-engineered ion thrusters was then transferred to NEXT's industrial partner, Aerojet, to produce higher fidelity hardware. This thruster, which is denoted with the PM label, along with an engineering model PMS was put through several tests including performance testing, environmental testing, and single string integration testing with the PPU. To ensure the PM design performs and wears similarly to

the GRC-engineered EM design, a short duration wear test was then performed. The objectives of this test were to characterize the thruster operation and performance over the test duration, identify any wear or performance changes from the EM design, and demonstrate extended operation of the PM thruster design and engineering model PMS. Testing of previous thrusters has shown that 1500 to 2000 hr of operation is sufficient to establish beginning of life changes and demonstrate initial trends. The findings from this wear test will be incorporated into current lifetime modeling and assessments.

This paper presents the results from the wear test using the NEXT PM1R ion thruster and engineering model PMS. A description of the test articles are discussed in the next section. This is followed by a description of the test support hardware, which includes the power console, external gas feed system, the vacuum facility, data acquisition system, and diagnostics. The test operating conditions are then described. Finally, wear test and post-test inspection results are presented for the thruster and the PMS, and the impact on the thruster service life is assessed.

Test Article

Thruster

Hardware Description

The engineering model thruster (previously labeled prototype model, or PM) used in the wear test is labeled PM1R, and is shown in Figure 1. The PM thruster design is functionally identical to the thruster developed by NASA (Ref. 22). The PM design improved upon the GRC thruster design with emphasis on surviving vibration and thermal environments and on reduced thruster mass. Manufacturability was also improved with this new design. The PM thruster design included innovative coatings to increase emissivity for enhanced thermal margin, more uniform ion optics aperture diameters with much shallower cusps, a 36 cm beam extraction diameter to reduce edge aperture erosion, and graphite discharge cathode keeper to mitigate keeper erosion. The PM1R thruster mass, including the cable harnesses, is 13.5 kg. The thruster input power throttling range is 0.5 to 6.9 kW, with thrust and specific impulse ranges of 26 to 236 mN and 1400 to 4200 s, respectively. A more detailed discussion of the PM thruster design can be found in Reference 23.

Test History

Prior to the wear test, the PM1/PM1R thruster was subjected to a number of performance and environmental tests. A summary of the PM1/PM1R operation prior to the wear test is given in Table 1 along with the amount of time the thruster was operated with high voltage. The PM1R thruster is a reworked version of the PM1 thruster that was initially performance tested in the summer of 2006



Figure 1.—Photograph of the NEXT PM1R ion thruster.

(Ref. 24). Subsequent environmental tests uncovered deficiencies in the thruster design (Ref. 25). These design deficiencies were resolved and the reworked thruster, labeled PM1R, was successfully performance acceptance tested during the summer of 2007. Following that test, PM1R was used for a thruster-PPU integration test. The thruster was then environmentally tested to qualification levels at JPL (Ref. 26). Environmental testing included vibration and thermal vacuum testing with thruster functional tests following each test to assess thruster functionality. The PM1R thruster successfully completed environmental testing and detailed results can be found in Reference 26. Immediately prior to the wear test, the thruster was used for a single string integration test, which is described in Reference 27.

TABLE 1.—PM1/R HISTORY PRIOR TO WEAR TEST OPERATION.

Thruster label	Test	Dates of operation	High voltage operational time, hr
PM1	Performance acceptance test	February 2 to 21, 2006	30.3
	Performance acceptance test	May 5 to 15, 2006	13.4
	Thermal development test	August 18 to September 8, 2006	36.7
	Characterization prior to and after vibration testing	September 18 to November 1, 2006	21.5
	Thermal vacuum test	November 8 to 15, 2006	28.5
PM1R—New DCA, NCA, plasma screen, same optics	Performance acceptance test	June 11 to 14, 2007	24.8
	PPU integration test	June 22 to 28, 2007	26.7
	Characterization prior to and after vibration testing	July 18 to August 10, 2007	23.3
	Thermal vacuum test	August 13 to 21, 2007	36.0
	Single string integration test	June 19 to September 9, 2008	177.5

Propellant Management System

Hardware Description

The propellant management system used for the wear test was an engineering model system. The overall design approach was developed by a NEXT integrated product team led by NEXT program's industrial partner Aerojet, who designed and manufactured the engineering model hardware. A schematic of the PMS is shown in Figure 2. The PMS is composed of High Pressure Assembly (HPA) and Low Pressure Assembly (LPA). The HPA reduces xenon tank pressure from a maximum expected operating inlet pressure of 18,600 kPa (2700 psia) to a regulated outlet pressure of 240 kPa (35 psia). The outlet pressure is regulated with proportional flow control valve (PFCV) using an outlet pressure transducer for feedback. The HPA includes a redundant PFCV and outlet pressure transducer for fault tolerance. A single HPA can provide flow to multiple LPAs for systems utilizing multiple thrusters.

The LPA provides independent flow control to each of the three thruster propellant inputs, labeled neutralizer, cathode, and main in Figure 2. During normal operation, each LPA branch flow rate is set by regulating the pressure to a heated porous plug, or thermal throttle, with a separate PFCV and pressure transducer. Thermal throttle temperature is controlled using a sheathed heater with a temperature sensor for feedback. As with the HPA, thermal throttle inlet pressure is regulated with a PFCV using a pressure transducer for feedback. The thermal throttle temperature is set to 75 °C and thermal throttle inlet pressures range from 77.9 to 189 kPa (11.3 to 27.4 psia) to achieve the commanded flow rates. To support fault tolerance in the design, the LPA design includes latch valves between the three branches of the LPA and the thermal throttle was designed for operation up to 400 °C. The thermal throttle design also incorporated a redundant heater and temperature sensor for fault tolerance.

Photographs of the NEXT engineering model HPA and LPA are shown in Figure 3 and Figure 4, respectively. The HPA's redundant PFCV and outlet pressure transducer were mass model mock-ups to reduce assembly cost. The LPA main flow branch can output a xenon flow rate of up to 50 sccm, while the cathode and neutralizer branches can output up to 6 sccm each. The HPA and LPA weigh 1.9 and 3.1 kg, respectively. These masses include each assembly's mounting plate, connectors, and component heaters used for the system integration and wear tests.

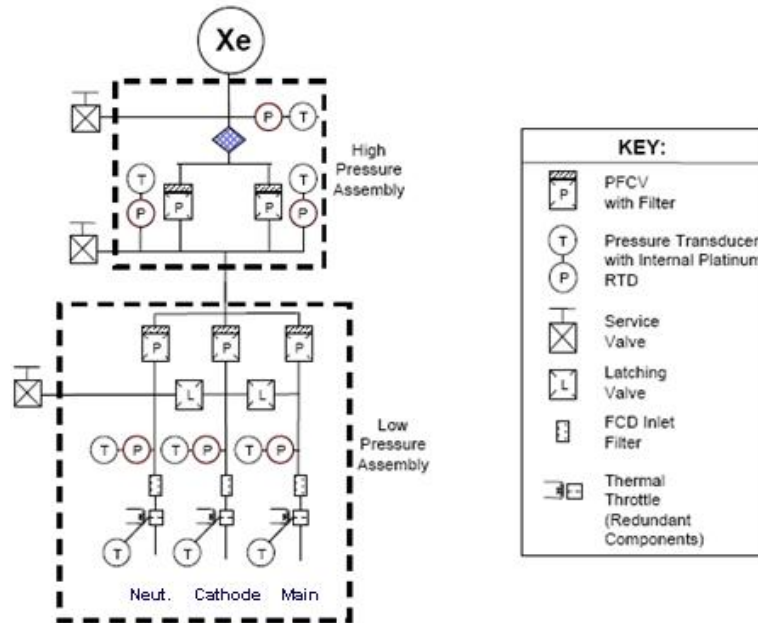


Figure 2.—Schematic of the NEXT PMS. The xenon tank is not included in the NEXT PMS development.



Figure 3.—Photograph of engineering model HPA.



Figure 4.—Photograph of engineering model LPA.

Test History

The engineering model HPA and LPA have completed environmental testing at qualification levels. Vibration testing was conducted in April of 2005. Thermal vacuum testing was conducted in May of 2007. Flow calibration checks were conducted prior to and following the vibration test and throughout the thermal vacuum test. Proof pressure tests, leakage checks, and electrical checks were conducted on the HPA and LPA prior to and following the vibration and thermal vacuum tests. The PMS successfully

completed environmental testing, and the results of these tests can be found in References 28 and 29. The PMS was also used for a single string integration test, which is described in Reference 27.

Test Support Hardware

Power Console

A power console similar to that described in Reference 30 powered the ion engine. This was also similar to the power consoles used in the two previous NEXT wear tests (Refs. 19 and 32). This power console utilized commercially available power supplies that allow for ion engine input powers of over 10 kW with beam power supply voltages of up to 2000 V.

External Gas Feed System

The PMS was integrated into a Xenon Feed System Equipment (XFSE) assembly, as shown on the schematic in Figure 5. The XFSE is ground test-support equipment and, therefore, not a part of the flight system. The XFSE was used to monitor the operation of the PMS during the wear test, but could also provide a secondary thruster gas feed system. The XFSE was divided into two systems. The external XFSE was located on atmospheric side of the vacuum facility. It included mass flow controllers for checking LPA flow rate calibrations and could independently provide flow to the thruster using mass flow controllers, thus allowing for thruster operation using a standard flow regulation configuration. The internal XFSE was located within the vacuum facility. It included manual and solenoid valves that allowed for configuration changes, such as thruster operation with and without the engineering model PMS. The internal XFSE included one HPA and one LPA, which represented a single thruster string PMS, as shown in Figure 5. The internal XFSE and PMS were covered with a polyimide foil for protection against back-sputtered material deposition. A photograph of the test setup is shown in Figure 6.

Tubing and components of the PMS and XFSE were wrapped with heater tape for a bake-out to remove air and adsorbed moisture on surfaces exposed to atmosphere. About twenty thermocouples were mounted on key PMS and XFSE components and were monitored and recorded by a separate data acquisition system throughout testing. To simulate pressure drops due to viscosity, the tubing leading from the LPA outlet to the thruster inlet included 3.5 m of 0.32 cm diameter \times 0.71 mm wall tubing, which is similar to the longest tubing length used with the Dawn ion thruster propellant management system.

For the wear test, a Digital Control Interface Unit (DCIU) Simulator, described in Reference 27, monitored and recorded all pressures, temperatures, and flows measured by the PMS and XFSE. The DCIU Simulator also monitored and recorded PMS component input currents and voltages other than those of the pressure transducers. For the PMS, the DCIU Simulator regulated HPA outlet pressure, LPA outlet flow rates, and thermal throttle temperatures, and controlled latch valve position and the selection of primary or redundant thermal throttle heaters. For the XFSE, the DCIU Simulator controlled and recorded telemetry from the mass flow controllers. A data acquisition computer was used to record the thruster voltages and currents separately as well as the total flow measured by the Main mass flow controller.

For the entire wear test, the PMS was operated in standard mode—that is, all thermal throttle temperatures were set to a constant 75 °C and the LPA thermal throttle inlet pressures were used to set the desired flow rates. Thermal throttle inlet pressures ranged from 77.9 to 189 kPa (11.3 to 27.4 psia) to achieve these flow rates. The HPA outlet pressure was set to the standard 241 kPa (35 psia) throughout the wear test. The valves on the XFSE were set to divert the flow from the xenon bottles through the XFSE main mass flow controller, as shown in Figure 5 and the flow controller's valve was fully opened. With this setup, the total flow rate to the PMS could be monitored by main mass flow controller. The inlet pressure to the HPA was 345 kPa (50 psia), which was the calibration pressure for the mass flow controller. The setup was the same as that used during the NEXT single string integration test (Ref. 27).

Vacuum Facility

The PM1R thruster and PMS, along with part of the XFSE, were installed in GRC's Vacuum Facility 5 (VF5). This vacuum facility has an inner diameter of 4.6 m and an overall length of 18.2 m. It is cryogenically pumped with internal cryogenic pumps for a total measured pumping speed of 260 kL/s with xenon and a base pressure of about 5×10^{-5} Pa (4×10^{-7} Torr). The facility also has a turbomolecular pump for the removal of lighter gases and a residual gas analyzer for monitoring gas partial pressures. Background pressures during full power thruster operation were within 4.5×10^{-4} Pa (3.4×10^{-6} Torr) and at low power operation were within 2.0×10^{-4} Pa (1.5×10^{-6} Torr), as measured by an internal ion gage located 41 cm below the centerline of and 25 cm behind the PM1R thruster.

There was a graphite target installed downstream from the thruster to protect the facility pumping system and minimize the backspattered material. The cylindrical walls of the facility were not covered for this test, leaving exposed stainless steel. Vacuum Facility 5 was selected because of its pumping speed and size, which was large enough to accommodate the PMS, the PM1R thruster, and associated thruster plume diagnostics.

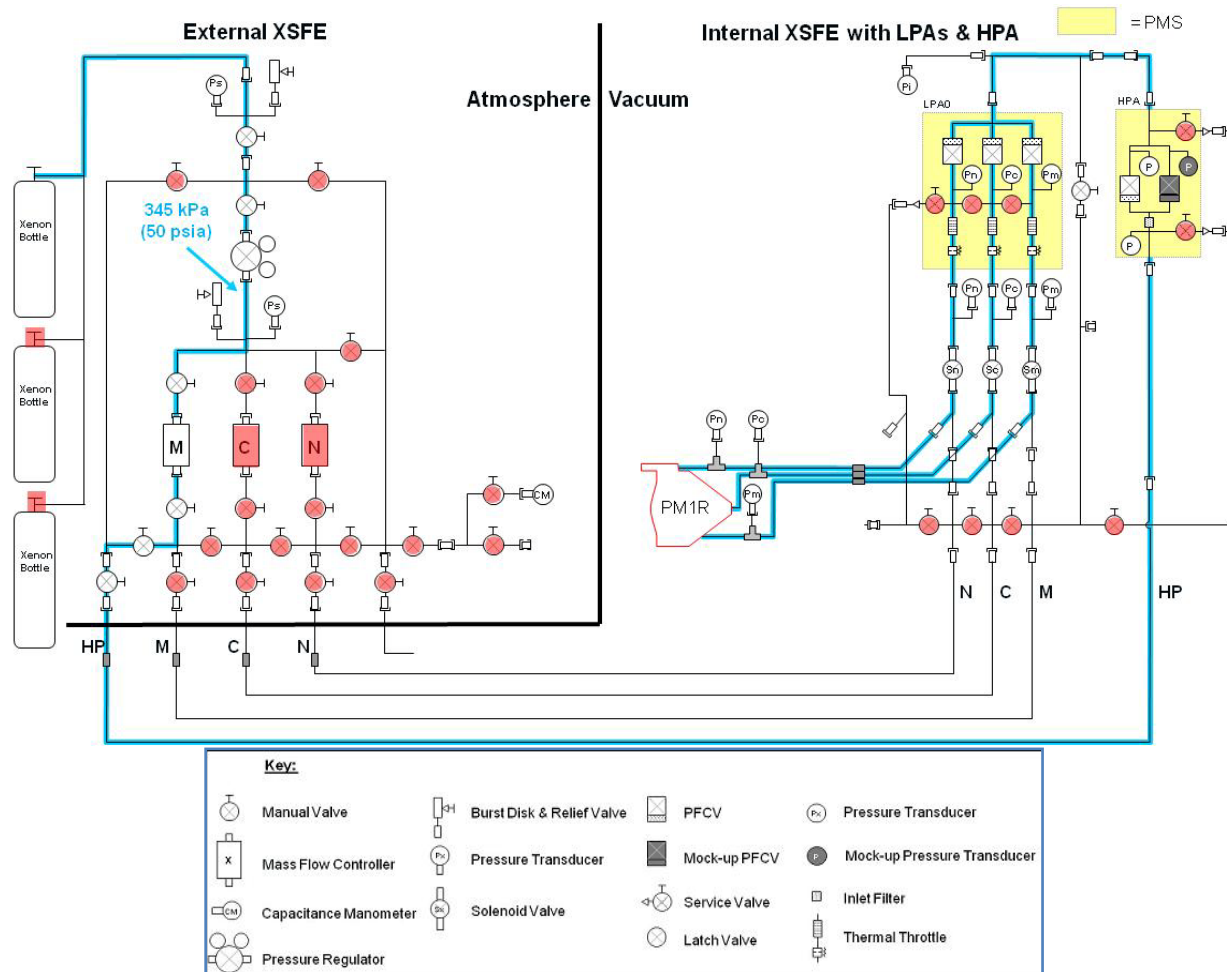


Figure 5.—Schematic of the PMS and XFSE. The HPA and LPA of the PMS used in this study are highlighted in yellow. Here, “M”, “C”, and “N” are the main, cathode, and neutralizer flow branches, respectively, and “HP” is the high pressure outlet of the internal XFSE that leads to the HPA inlet. The flow path from the xenon bottle is shown in blue. A red-tinted valve indicates that it was closed during the wear test. Although all three xenon bottles were used during the test, only one bottle at a time was opened.

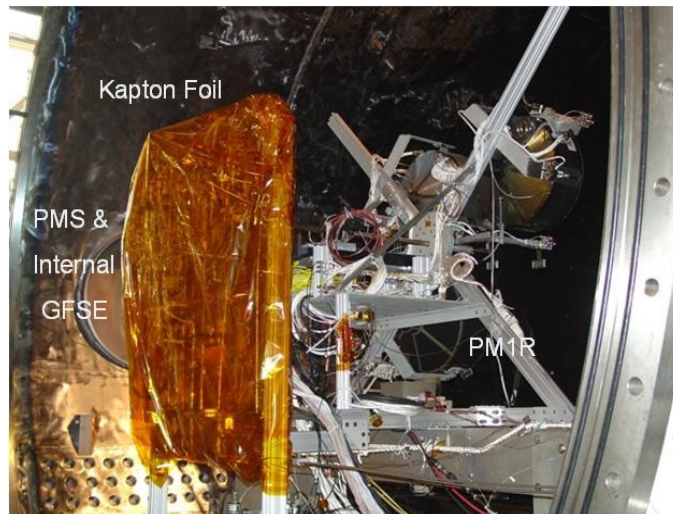


Figure 6.—Photograph of the PMS and internal XFSE mounted in VF5 prior to the start of the wear test. The location of the PM1R thruster is also shown.

Diagnostics

A computerized data acquisition and control system (DACS) was used to monitor the ion engine and facility operations to control the power console. Data was sampled at a frequency range of 10 to 20 Hz and was stored once per minute. Ion engine currents and voltages were measured with current shunts and voltage dividers, respectively, and recorded. Facility pressure and total mass flow to the ion engine were also sampled and recorded. The individual flows were recorded by the DCIU as previously mentioned. This DACS is of the same design as the two previous NEXT wear tests (Refs. 19 and 32).

Ion beam diagnostics consisted of circular planar probes on a two-axis probe motion system for measuring beam current density. There were a total of six planar probes with a 1 cm² circular current-collecting area. Two of these probes passed directly in front of the thruster, with one passing through the geometric center of the ion optics. To measure beam current density profiles, the probes were biased negative with respect to beam plasma potential to repel electrons and are grounded through separate resistors that act as shunts to measure collected currents.

Operating Conditions and Performance Tests

The NEXT system is designed for applications using power from solar arrays. In order to satisfy that application, the NEXT system has to operate over a wide range of input powers that range from 0.5 to 6.9 kW. The throttle table corresponding to this range is shown in Table 2. For the PM1R wear test, the majority of thruster operation is at the throttle point with the least operational lifetime (Refs. 15 and 16). This is at full power where the rate of groove erosion on the ion optics is greatest. Towards the end of the wear test, the thruster was operated at the lowest power to include the extremes of the throttle table. All thruster operation with beam extraction (i.e., high voltage operation), including performance tests, was included in the ongoing duration reported.

The wear test was interrupted after 43 hr for PPU-thruster testing related to the single string integration testing. High voltage operation totaling 23.1 hr with the PPU was included in the total wear test hours.

Throughout the wear test, performance tests were conducted on the engine and its components. The throttle points corresponding to the engine performance tests, which included measurements of engine operating parameters and calculated engine performance, are listed in Table 2. Component performance assessments were periodically made on the discharge chamber, ion optics, and neutralizer. Ion optics performance included electron backstreaming and perveance. Neutralizer performance included measuring peak-to-peak voltages at various flows to determine the transition from spot-to-plume mode.

TABLE 2.—SELECTED NEXT ION THRUSTER THROTTLE TABLE POINTS VERSION 9
INCLUDING WEAR TEST PERFORMANCE OPERATING CONDITIONS

[Full-power wear test conditions in bold.]

Nominal power in, kW	Beam current, A	Beam voltage, V	Accelerator voltage, V	Main flow, sccm	Discharge cathode flow, sccm	Neutralizer cathode flow, sccm	Neutralizer keeper current, A
6.83	3.52	1800	-210	49.6	4.87	4.01	3.00
4.68	3.52	1180	-200	49.6	4.87	4.01	3.00
5.27	2.70	1800	-210	37.6	4.26	3.50	3.00
3.61	2.70	1180	-200	37.6	4.26	3.50	3.00
4.00	2.00	1800	-210	25.8	3.87	2.50	3.00
2.77	2.00	1180	-200	25.8	3.87	2.50	3.00
2.43	1.20	1800	-210	14.2	3.57	3.00	3.00
1.70	1.20	1180	-200	14.2	3.57	3.00	3.00
1.11	1.20	679	-115	14.2	3.57	3.00	3.00
0.656	1.20	300	-525	14.2	3.57	3.00	3.00
0.529	1.00	275	-500	12.3	3.52	3.00	3.00

Results and Discussions

The NEXT PM1R engine accumulated 1680 hr of beam extraction during which 30.5 kg of xenon was processed. The PMS provide xenon to the thruster throughout the entire wear test. Full power wear test operation was conducted during the first 1359 hr of testing, which included performance testing. The remainder of the wear test is at the low power throttle point of 1.0 A beam current and 275 V beam power supply voltage, with the exception of 19.9 hr of operation at 1.2 A beam current and 679 V beam power supply voltage at hour 1634 in the wear test to allow for comparisons with the LDT. Performance test data will be reported as discreet points throughout this paper. The measurement uncertainties are the same as previous thruster tests and a discussion of these and thruster-to-thruster dispersions are given in Reference 31. A complete breakdown of the hours on the engine for its multiple operating points during the wear test and from the beginning of life, which is the wear time on the optics, is shown in Table 3. During the wear test, the discharge cathode operated for 1704 hr and the neutralizer cathode operated for 1709 hr.

Several ion engine performance tests were conducted throughout the wear test. The PMS was also used for the performance tests. There were a total of 24 test interruptions, which are described in Table 4 along with the cause of interruption. The only interruption related to thruster operation was after 437.5 hr of operation. After this interruption, the thruster restarted without issue. This interruption will be described under discharge chamber test results. The test was terminated voluntarily and the thruster was removed for inspection.

TABLE 3.—PM1/1R HIGH VOLTAGE TIME
[The shaded cells indicate wear test operating throttle points.]

BOL input power, W	Beam voltage, V	Beam current, A	Time from thruster BOL, hr	Wear test time, hr
530	275	1.00	301.4	276.9
1110	679	1.20	63.2	22.7
1700	1179	1.20	27.6	9.9
2430	1800	1.20	36.7	13.6
2770	1179	2.00	35.5	5.3
4000	1800	2.00	48.3	10.8
3200	1021	2.70	12.1	5.3
5270	1800	2.70	33.0	11.5
4680	1179	3.52	68.8	5.8
6830	1800	3.52	1436.2	1311.5
660-6790	Remaining 25 throttle points		35.8	6.3

TABLE 4.—WEAR TEST INTERRUPTIONS

HV time, hr	DCA time, hr	NCA time, hr	Wear test interruption cause
7.2	10.1	10.6	DACS debugging
11.6	14.9	15.5	NEXT PPU test
29.9	34.6	35.4	NEXT PPU test
40.8	47.6	48.6	Vacuum facility lost vacuum ~1 torr maximum pressure
71.4	85.7	87.9	DCIU reached maximum recording file size
72.5	87.1	89.4	DCIU input power interrupted
154.2	169.0	171.4	Bad discharge power supply
155.2	170.3	172.8	Bad discharge power supply
156.1	171.4	174.0	Vacuum facility lost vacuum ~1 torr maximum pressure
287.0	302.6	305.4	Flow limit on DACS incorrectly set
327.4	343.4	346.8	Vacuum facility lost vacuum ~1 torr maximum pressure
437.5	454.6	458.3	Beam current low
650.7	668.1	671.8	Thruster off to switch Xe supply bottles
892.8	910.4	914.2	Noise in DAQS resulted in high Jhv
893.3	911.1	915.0	Faulty facility signal
938.2	956.5	960.6	Beam console supply fault
1058.1	1076.7	1080.8	Faulty facility signal
1227.5	1246.4	1250.6	Vacuum facility lost vacuum ~1 torr maximum pressure
1359.1	1379.7	1384.1	Beam console supply fault
1475.6	1496.4	1501.1	Voluntary shutdown to allow for cool ignition (1.0 A, 275 V)
1495.8	1517.2	1522.0	Voluntary shutdown to allow for cool ignition (1.0 A, 275 V)
1516.0	1537.4	1542.2	Voluntary shutdown to allow for cool ignition (1.0 A, 275 V)
1537.6	1559.2	1564.1	Voluntary shutdown to allow for cool ignition (1.0 A, 275 V)
1675.7	1697.6	1702.6	Voluntary end of test shutdown

Test Results

Vacuum Facility

The facility pressure measured near the ion engine and corrected for xenon is shown in Figure 7. The vacuum facility suffered four failures where the background pressure rapidly increased to approximately 1 torr on each occasion. These occurred at hours 41, 156, 327, and 1228 during the wear test. These rapid pressure increases following facility pumping system shutdowns were due to a liquid nitrogen leak near the cryopanel. This leak was not evident in the background pressures since it froze out rapidly on the cryogenically cooled panels. However, when the cryogenic system was interrupted, it led to rapid and high background pressures. After the first failure at 41 hr, the vacuum chamber was opened for an unrelated facility issue. The vacuum chamber was then closed and not opened until the completion of the test. The panel related to the liquid nitrogen leak was removed from the system after the fourth facility failure, with no adverse effects to the tank pressure.

The vacuum facility had a graphite target, but the walls were exposed stainless steel. Post-test samples indicated that the backsputter rate was 5.8 $\mu\text{m}/\text{kh}$. The samples also showed that a substantial portion of the material coming back to the thruster was stainless steel, likely from the exposed facility walls, in addition to carbon. The backsputter rate at 1.0 A beam current and 275 V beam power supply voltage was at a significantly lower rate of 0.09 $\mu\text{m}/\text{kh}$.

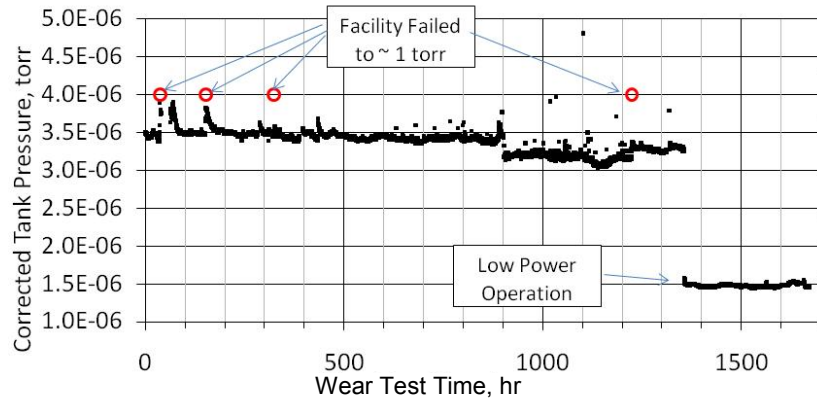


Figure 7.—Vacuum facility pressure corrected for xenon as a function of time.

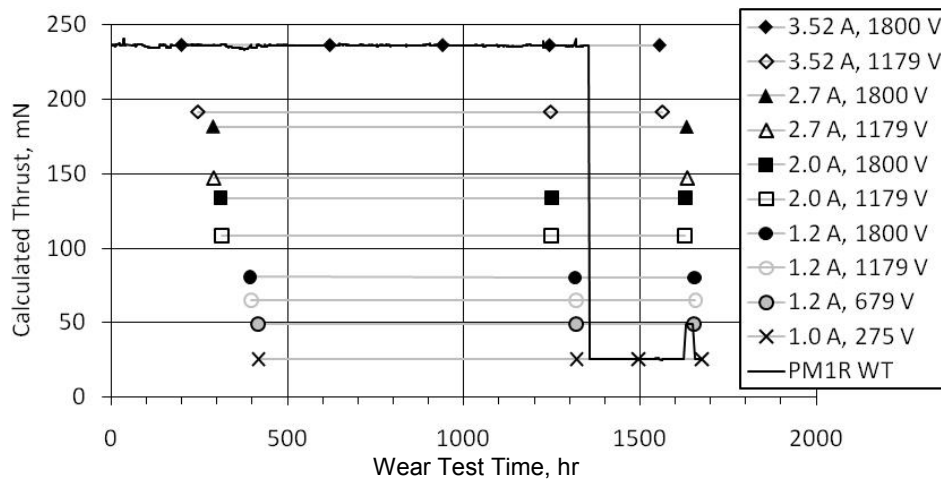


Figure 8.—Calculated thrust as a function of time. The legend lists corresponding beam currents and beam power supply voltages.

Ion Engine Performance

Engine performance parameters of interest to mission planners include thrust, input power, specific impulse, and thrust efficiency. Calculated thrust, input power, specific impulse, and thrust efficiency as a function of time are shown in Figure 8 to Figure 11 for operating points throughout the throttle table. Ingested mass flow due to facility background pressure was included in the total mass flow rate to the engine for determining specific impulse and thrust efficiency.

The average calculated thrust, input power, specific impulse, and thrust efficiency at full power were 236 mN, 6.85 kW, 4184 s, and 0.707, respectively, and at low power were 25.5 mN, 0.53 kW, 1425 s, and 0.337, respectively. The beam current variations were as much as +0.07/−0.05 A at full power and +0.02/−0.02 A at low power. The beam current variation was primarily due to a lack of an automated closed loop control of beam current on discharge current. Variations in other parameters were predominantly due to changes in beam current. So, for example, when the beam current decreased, the input power and thrust decreased, leading to decreases in specific impulse and thrust efficiency as well. Regardless, maximum variations throughout the test of these full power values were +5/−3 mN, +0.14/−0.09 kW, +69/−64 s, and +0.011/−0.010, respectively, and for low power +0.4/−0.6 mN, +0.02/−0.01 kW, +40/−32 s, and +0.006/−0.007, respectively. These variations are comparable to previous wear tests (Refs. 19 and 32).

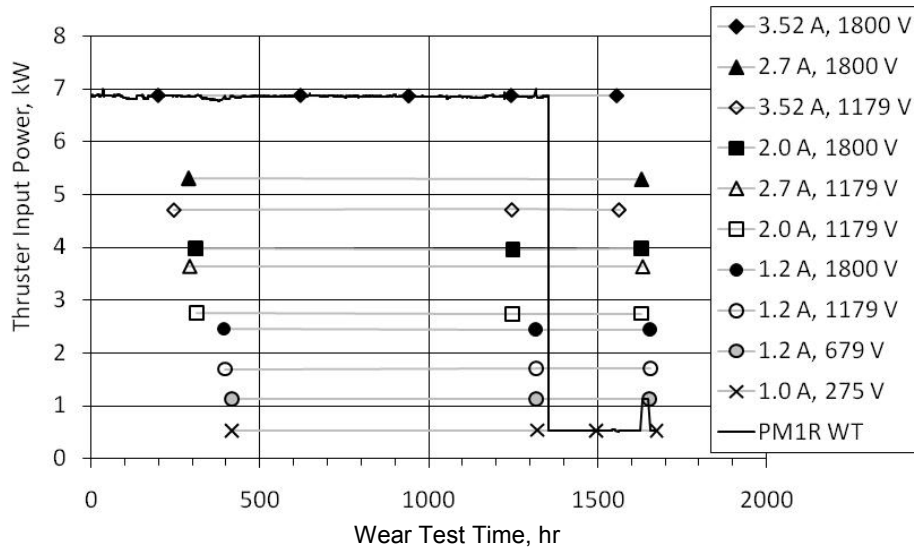


Figure 9.—Thruster input power as a function of time. The legend lists corresponding beam currents and beam power supply voltages.

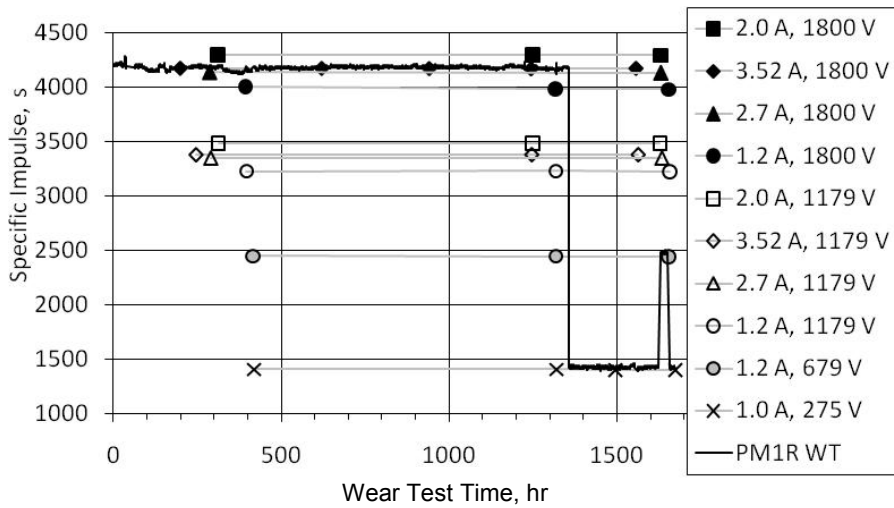


Figure 10.—Specific impulse as a function of time. The legend lists corresponding beam currents and beam power supply voltages.

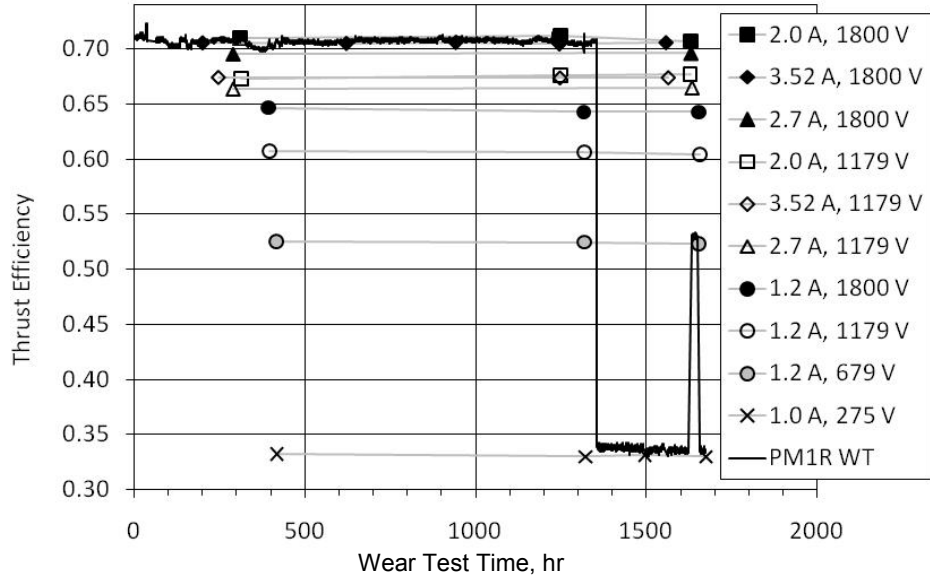


Figure 11.—Thrust efficiency as a function of time. The legend lists corresponding beam currents and beam power supply voltages.

Thruster Discharge Chamber

Discharge current and voltage as a function of time are shown in Figures 12 and 13, respectively. Average discharge currents and voltages at full power were 19.4 A and 23.9 V, respectively, and at low power were 8.12 A and 26.0 V, respectively. The discharge current and particularly the discharge voltage exhibited slightly larger variations than previous NEXT wear tests (Refs. 19 and 32). Previous NEXT wear tests reported that the discharge current and voltage variations were generally ± 3 percent, and the variations for the PM1R wear test are closer to ± 3.5 percent at full power (Refs. 19 and 32). At low power, the variations are typically within ± 3 percent. Some of the larger variations were due differences in thruster startup procedures. Ion beam extraction occurred 15 min following discharge ignition for this wear test. In previous wear tests, the beam extraction was at least 1 hr after ignition and yielded a warmer thruster closer to thermal steady state conditions.

As with other wear tests, the discharge current trended higher with time. The current increased about 0.7 A in the first 500 hr of testing and then leveled off. The discharge voltage trended downward in the first few hundred hours of testing. During that timeframe, the voltage decreased gradually from 24.6 V down to 24.0 V three times. In contrast, after the first 400 hr, the voltage periodically dropped abruptly about 0.5 V, which was frequently associated with a thruster shut down where it had sufficient time to cool, only to rise back over the next 100 hr. These voltage drops were seen early in the LDT, but with a magnitude of 0.3 V (Ref. 32). It is uncertain if the NSTAR thruster had the same type of variations, but it did exhibit short-term voltage variations of ± 0.6 V (Ref. 6).

The discharge losses with time are shown in Figure 14. At full power, the discharge losses generally increased 1 W/A from the beginning of test to end of test, with periodic variations between 129 W/A to 133 W/A (i.e. a bandwidth of 4 W/A or 3 percent), with the discharge losses dropping rapidly at times and then slowly increasing. Prior to the wear test, the discharge losses had increased quickly after the first performance acceptance testing of PM1R. The discharge losses initially tested on PM1R were 126 W/A, but after about 60 hr of operation on a new cathode, the losses increased to 129 W/A, which is what they were at the beginning of the wear test. After a few hundred hours into the wear test, changes in discharge losses strongly tracked changes in discharge voltages. Closer examination of the first two thousand hours of the LDT reveals that there were similar, but smaller, fluctuations in discharge losses from 123 to 125 W/A (i.e., a bandwidth of 2 W/A or 2 percent) along with a slight trend from 122 to 125 W/A at the end of 2,000 hr (Refs. 18 and 32).

While these changes are small, it is speculated that some of these variations could be due to changes in cathode thermal losses. The hollow cathode contains a barium impregnated porous cylindrical insert inside of a cylindrical tube. As the cathode operates, barium is released from the insert and migrates out of the insert and into the gap between the insert and the tube. While initially the heat loss out of the insert to the tube is primarily through radiation heat transfer, the barium provides a thermally conductive path out of the insert and into the tube, which increases the losses. Thermal modeling of the cathode has indicated an increase of 10+ W can occur from the increased thermally conductive losses, which is of the same order of magnitude of the discharge loss variations seen in the NEXT thruster. When the thruster is shut off and the cathode cools, the gap expands and enables a break in the barium conductive path, only to be reestablished over time during further operation. Only a small amount of barium would be needed to affect the thermal conduction away from the insert. This mechanism would explain why the ion engine can rapidly become more efficient following ignition and then take 50 to 100 hr to settle into higher discharge losses. These discharge loss step changes occurred not only at times of cold cathode restarts, but also at times during operation. It should also be noted that after several thousand hours, the variations were no longer seen in the LDT, which could correspond to sufficient barium in the gap causing it to maintain thermal contact.

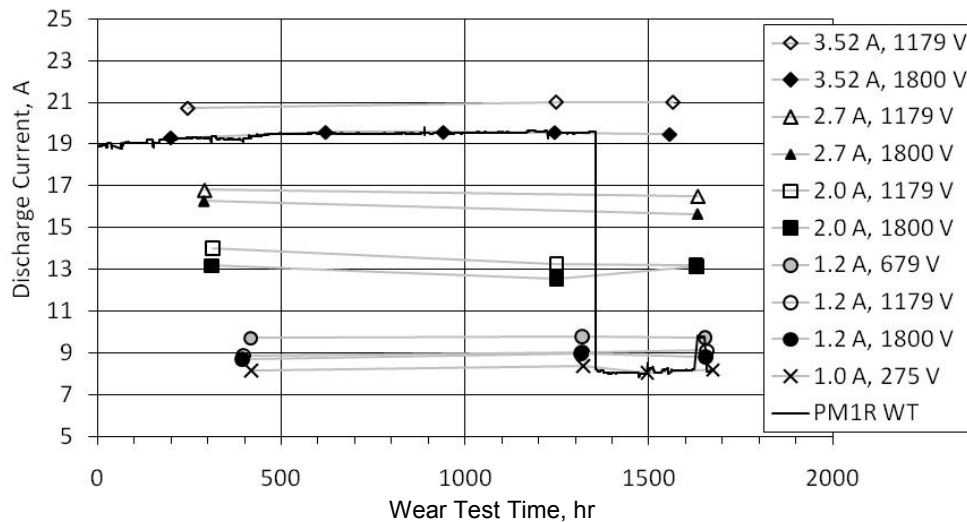


Figure 12.—Discharge current as a function of time. The legend lists corresponding beam currents and beam power supply voltages.

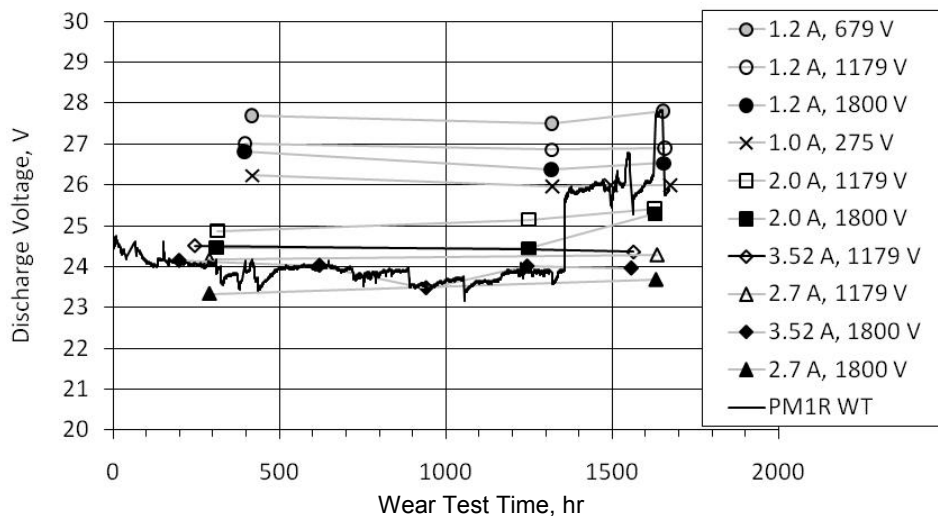


Figure 13.—Discharge voltage as a function of time. The legend lists corresponding beam currents and beam power supply voltages.

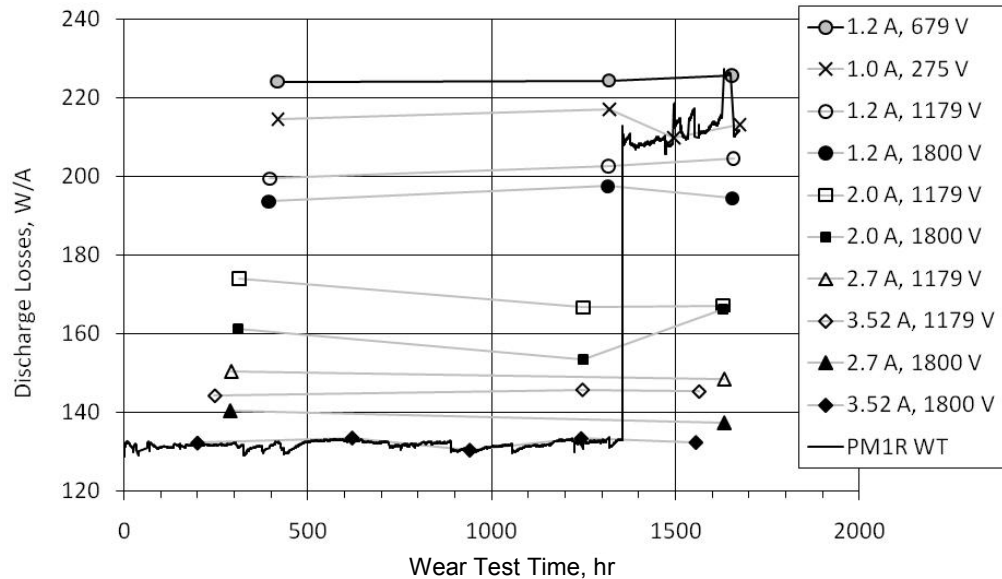


Figure 14.—Discharge losses as a function of time. The legend lists corresponding beam currents and beam power supply voltages.

This phenomenon could also explain behavior causing the test shutdown after 437.5 hr of operation. The shutdown was initiated by the DACS when the beam current immediately dropped, while the thruster performance increased. Prior to this event, the thruster was operating with a beam current of 3.5 A, a discharge current of 19.4 A, and a discharge voltage of 23.7 V, which corresponds to 131 W/A in discharge losses. The recording rate was once a second, and the thruster shifted performance in 1 sec. The thruster shutdown because the low beam current, 3.3 A, triggered a limit violation in the DACS software. The discharge current remained unchanged since it was a controlled parameter, but the discharge voltage dropped to 22.0 V, yielding a discharge loss of 129 W/A. The thruster immediately became more efficient, possibly due to the barium breaking contact and lessening the thermal loss out of the insert. Following the test interruption, the thruster impedance was checked and found to be nominal. After the thruster was restarted, it initially operated at 129.2 W/A of discharge losses. Over the next 90 hr, the discharge losses returned to 133 W/A.

The discharge keeper voltage is shown in Figure 15. The discharge keeper voltage trended downward over the test duration from 5.0 to 4.5 V, with a shorter term variations of 0.8 to 1.5 V. Several of the downward “spikes” were associated with engine restarts. The LDT showed an initial downward trend of 0.3 V with similar short term variations of 0.5 to 1.0 V (Ref. 35). The discharge keeper voltages exhibited similar behavior between the two tests.

These trends in the discharge performance during the wear test are consistent with the life assessments and performance expectations to date. The discharge cathode ignition times during the wear test were all nominal. There were a total of 40 ignitions of the discharge cathode and all but one was 5 min or less. The first DCA ignition was the only exception at 6 min and 44 sec.

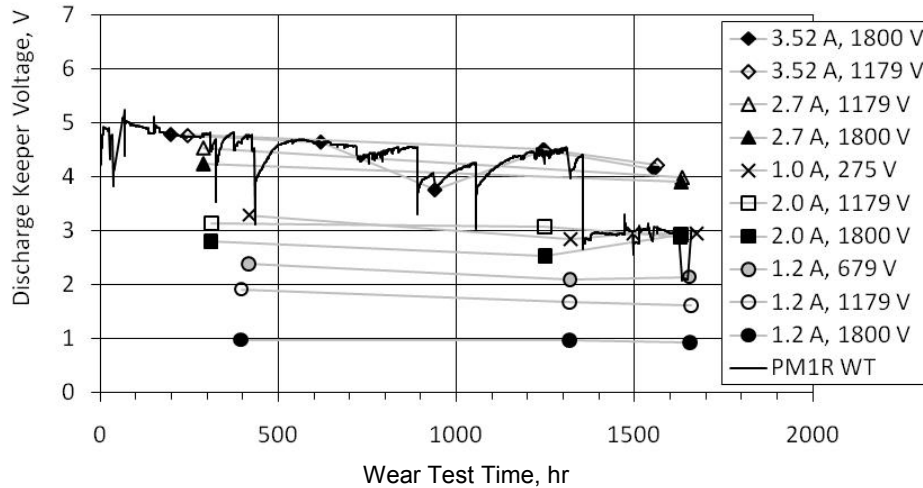


Figure 15.—Discharge keeper voltage as a function of time. The legend lists corresponding beam currents and beam power supply voltages.

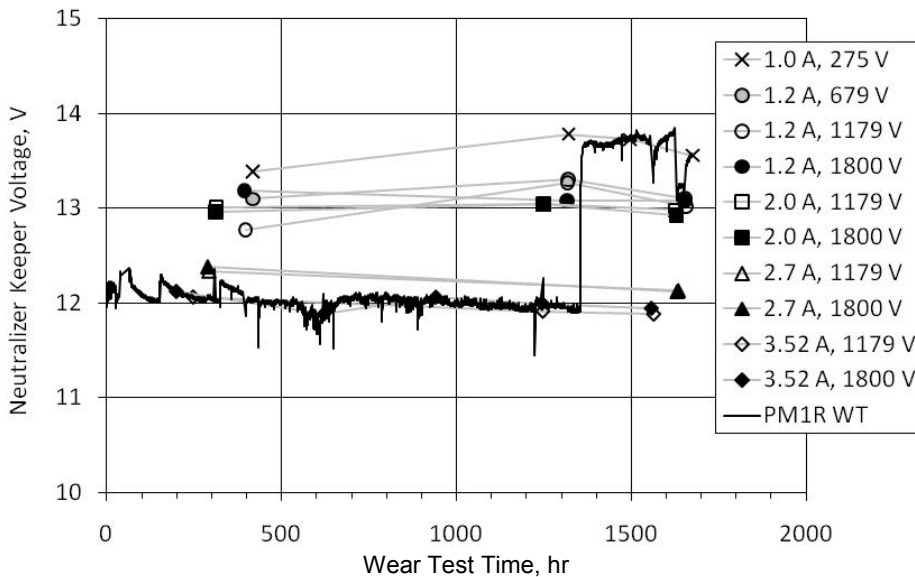


Figure 16.—Neutralizer keeper voltage as a function of time. The legend lists corresponding beam currents and beam power supply voltages.

Thruster Neutralizer

Neutralizer keeper voltage as a function of time is shown in Figure 16. The average neutralizer keeper voltage at full power was 12.0 V and at low power was 13.7 V. This is different than previous NEXT tests (Refs. 19 and 32), because the cathode-to-keeper gap was changed on the PM thrusters to allow additional spot-to-plume margin (Ref. 24). The maximum variations at full power were +0.9/−0.6 V and +0.2/−0.5 V at low power. The neutralizer keeper voltage followed a similar trend as the discharge voltage during the first 200 hr by starting at a higher voltage and decreasing. This is likely due to the facility failures and the resulting exposure of the cathodes to the higher pressures. The neutralizer keeper voltages exhibited voltage “spikes” corresponding to engine restarts, which are similar to previous NEXT and NSTAR neutralizer behavior (Refs. 6, 8, 18, 19, and 33). The increased bandwidth in voltages after 500 hr of operation also occurred during periods of increased engine recycling. During engine recycling, the neutralizer cathode emission current is changing from 6.5 to 3.0 A, which will change the neutralizer keeper voltage.

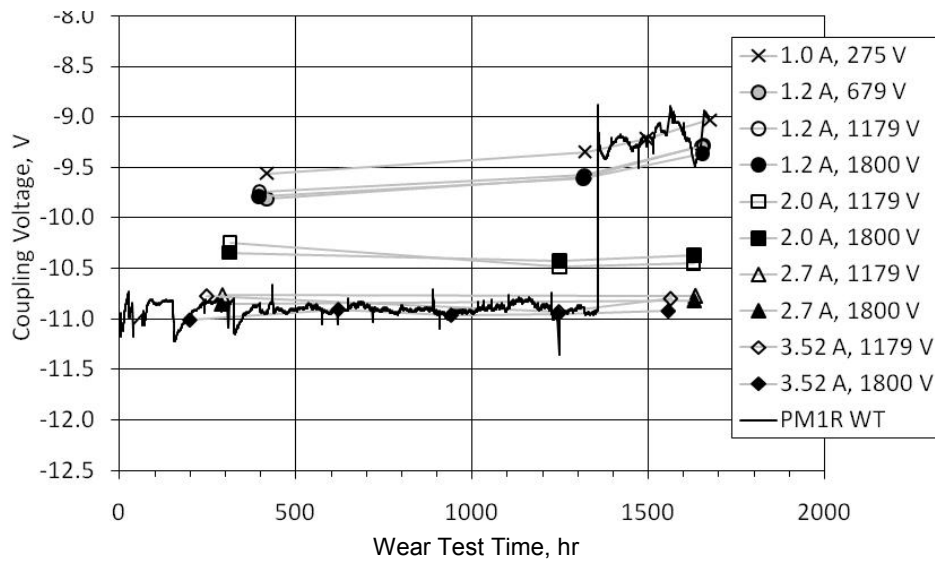


Figure 17.—Coupling voltage as a function of time. The legend lists corresponding beam currents and beam power supply voltages.

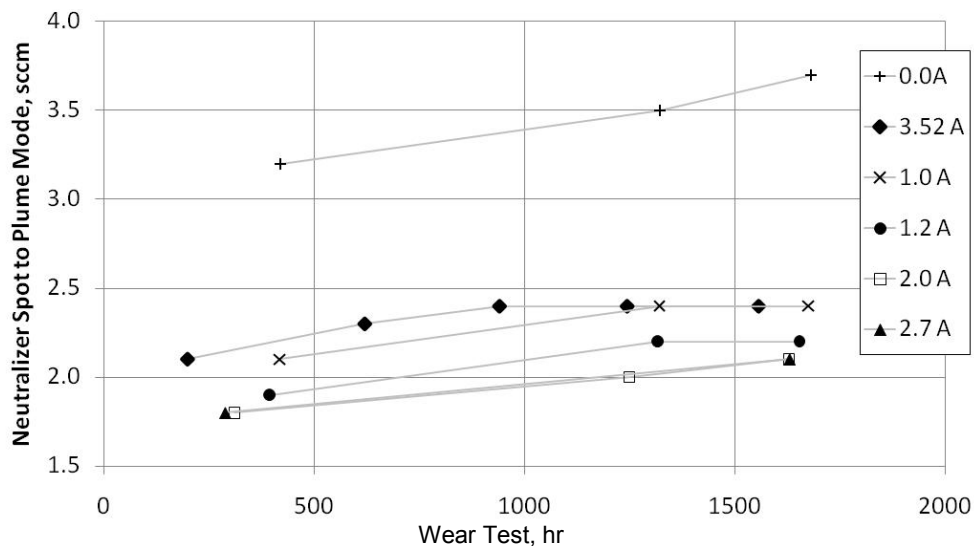


Figure 18.—Transition to plume mode neutralizer flow as a function of time at various beam currents.

Coupling voltage, which is the measure of neutralizer cathode potential relative to vacuum facility ground, is plotted in Figure 17 as a function of time. The mean coupling voltage at full power was $-10.9 \text{ V} \pm 0.2 / -0.5 \text{ V}$ and at low power was $-9.2 \text{ V} \pm 0.3 \text{ V}$, both of which are similar to previous tests. The neutralizer keeper and coupling voltages indicate no neutralizer performance degradation.

Figure 18 shows the neutralizer flow at the transition from spot to plume modes as a function of elapsed test duration for multiple beam currents. Spot mode is characterized by low voltage oscillations, while plume mode is described by large fluctuations that can lead to reduced cathode life. Following the NSTAR criterion, plume mode operation is reached when peak-to-peak neutralizer keeper voltage oscillations exceed 5 V. The flow for the onset of plume mode increased for all beam currents over the test duration. The flows at onset of plume mode increased by 0.2 to 0.3 sccm over the duration of the test for all beam currents apart from discharge only operation where the flows increased by 0.5 sccm. An inspection following the wear test revealed a leak just upstream of the thruster in the neutralizer line that

was greater than 5×10^{-4} sccm on xenon. No leak was found prior to the wear test. This leak adds uncertainty to the measurements and will be further quantified after the PM1R is operated again with no leaks in the line. Even though a leak was found in the PM1R wear test, the changes in flows are consistent with that of the LDT, which increased by 0.3 sccm during the first 2000 hr.

The neutralizer was ignited 50 times during the wear test with no ignition exceeding 4 min. The neutralizer on the PM1R engine has performed within family of all NEXT neutralizers with the exception of performance changes due to the intentional increase in the cathode-to-keeper gap.

Thruster Ion Optics

Accelerator currents as a function of time from performance data covering the throttle table are plotted in Figure 19. The “spikes” in the accelerator current at full power correlate with engine recycles. The mean value at full power was 12.7 mA. The slight drop in current at ~900 hr corresponded to a drop in facility pressure as can be seen in Figure 7. The higher current at the beginning of the test also corresponded to a higher facility pressure. The mean value of the accelerator current at low power was 2.2 mA. Other than variations due to recycles or facility pressure, the accelerator current showed negligible variation with time. These results are consistent with the previous NEXT wear tests (Refs. 19 and 20), and showed less initial variation than NSTAR engine accelerator currents that started higher than normal and required up to 1500 hr to decrease to nominal values (Refs. 6 and 33).

Total engine recycles and recycle rate as a function of time are plotted in Figure 20. In the first 400 hr of testing the recycle rate was quite low and generally below 1 recycle/hr. From 400 to 900 hr of testing, the recycle rate dramatically rose to 9.5 recycles/hr. During this timeframe, high potential impedance measurements between the grids indicated that the recycles were likely due to debris between the grids. The debris source was likely the excessive amount of backsputter material from the stainless steel chamber walls. Post-test inspections showed that surfaces that were grit-blasted effectively contained the backspattered material, but surfaces like the PM1R front mask, which was not grit-blasted, spalled easily. The spalled material likely fell into the grids and into the intergrid region through an accelerator aperture during the test. The material appeared to clear after hour 900 when the recycle rate dropped to about 2 recycles/hr.

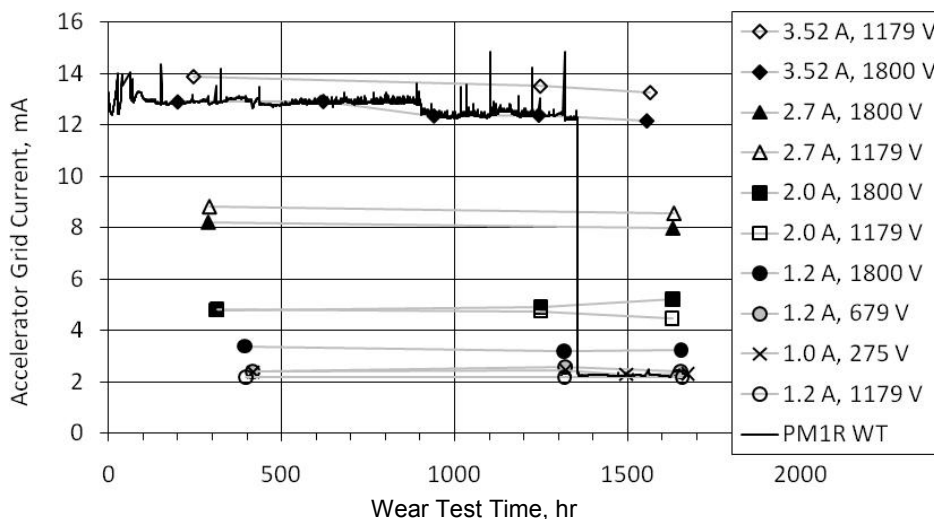


Figure 19.—Accelerator current as a function of time. The legend lists corresponding beam currents and power supply voltages.

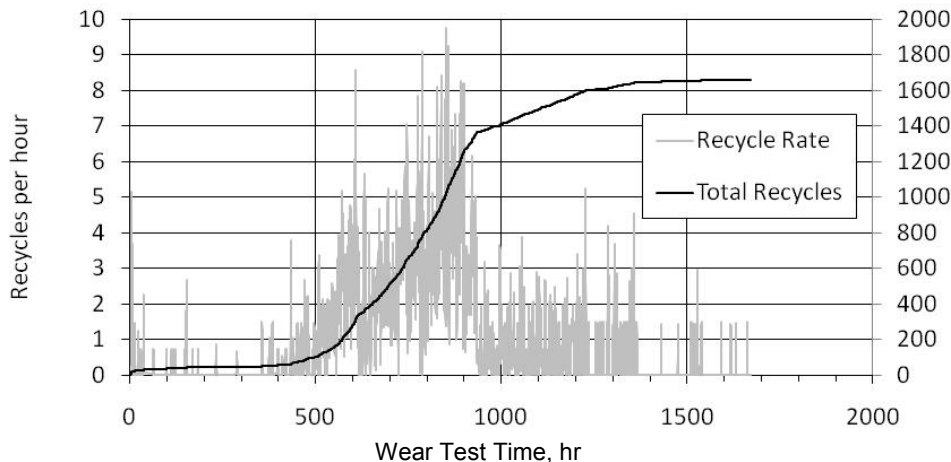


Figure 20.—Total recycles and recycle rate as a function of time. Recycle rate is the slope of the total recycles versus time over a 15 hr period.

Perveance limits and electron backstreaming limits throughout the wear test are shown in Figure 21 and Figure 22, respectively. Perveance limits were determined from plots of accelerator currents as a function of total voltage where the slope was -0.02 mA/V . Here, the total voltage is defined as the sum of the beam power supply voltage and the absolute value of the accelerator voltage. Electron backstreaming was determined by lowering the magnitude of the accelerator grid voltage until the indicated beam power supply current increased by 1 mA due to backstreaming electrons.

Throughout the throttle table, the perveance limits did not change beyond the accuracy of the measurement. The maximum measured change was 20 V. Perveance measurements taken in the first 2000 hr of the LDT showed a bandwidth of $\sim 50 \text{ V}$ at full power with no trend (Ref. 35).

The electron backstreaming limits showed negligible change throughout the wear test. This is consistent with LDT, with the optics of the same fidelity and construction as PM1R, where negligible changes were seen in the first few thousand hours (Ref. 35).

Radial beam current density profiles were measured as close as 45 mm downstream from the geometric center of the ion optics. Regarding beam current density measurements, no attempt was made to repel charge-exchange ions from the probe or to account for secondary electron emission due to ion bombardment. Integration of the radial beam current density profiles (assuming azimuthal symmetry) typically yield beam currents higher than the measured beam with the possible sources of error are discussed in Reference 34.

Post-test radial beam current density profiles are shown in Figure 23 taken at 45 mm downstream of the ion optics. Beam current density profiles did not change significantly during the wear test. Variations in peak beam current density as a function of time at full power are shown in Figure 24. Full power peak beam current densities at this axial location varied between 4.22 to 4.31 mA/cm^2 . The resulting ion engine beam flatness parameter (i.e. the ratio of average-to-peak ion current density) ranged from 0.81 to 0.83 throughout the wear test at full power. The beam density profiles also indicate no degradation in the performance of ion optics or the discharge chamber.

The PM1R ion optics performance throughout the wear test did not show any degradation in performance and are consistent with the LDT EM3 ion optics. Both of these wear tests are consistent with the service life assessments to date.

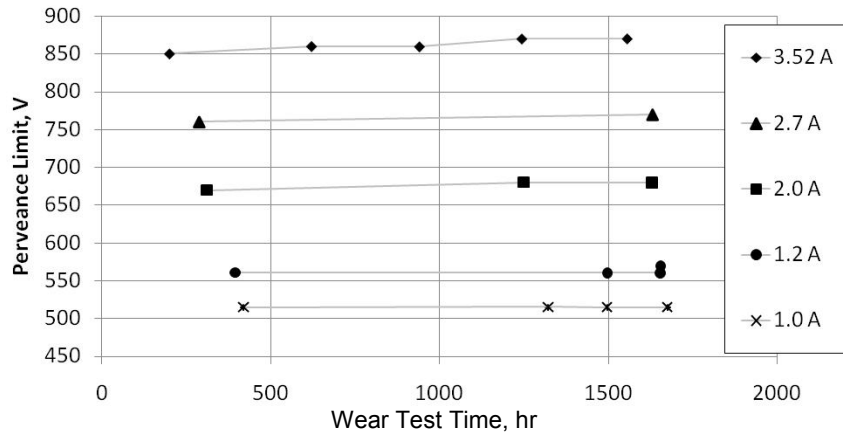


Figure 21.—Perveance limit as a function of time. The legend lists corresponding beam currents.

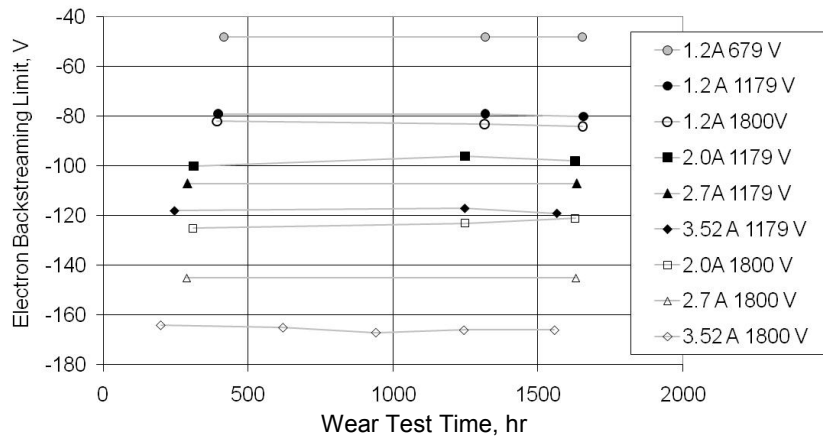


Figure 22.—Electron backstreaming as a function of time. The legend lists corresponding beam currents and beam power supply voltages.

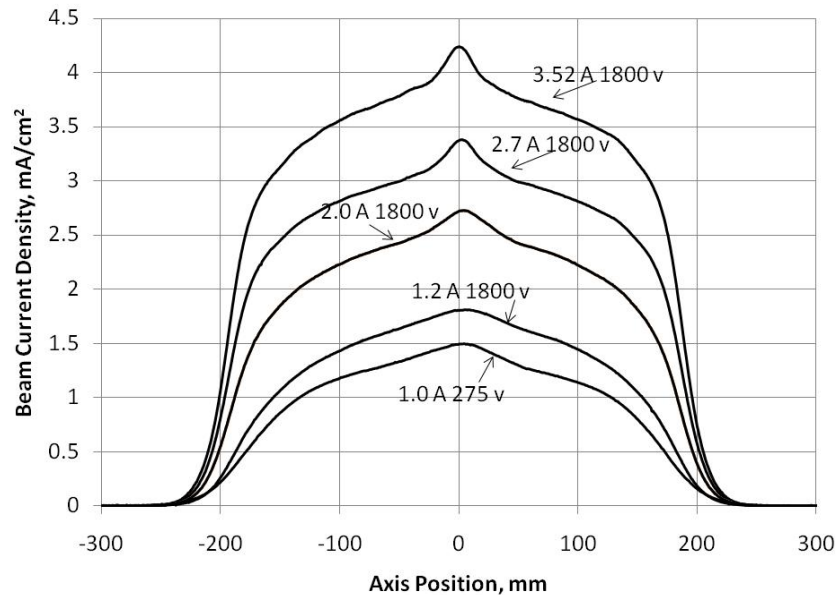


Figure 23.—End-of-test radial beam current density profiles. All densities were measured 45 mm downstream of the ion optics center.

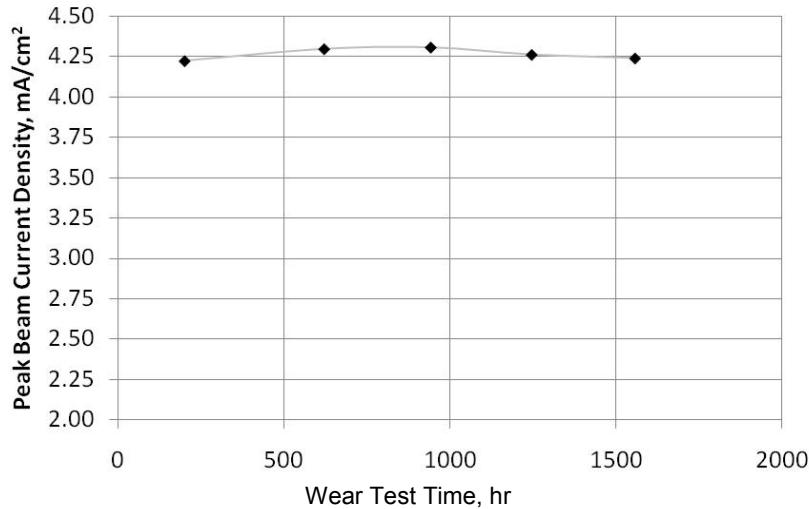


Figure 24.—Peak beam current density as a function of time at full power. All densities were measured 45 mm downstream of the ion optics' center.

Propellant Management System

The total PMS flow rate was monitored by the external XFSE main mass flow controller, as shown in Figure 5. The total PMS flow rate measured throughout the wear test is compared to that measured by the main mass flow controller in Figure 25. The main mass flow controller uncertainty was ± 1.0 percent for the full power flow rates during the first 1359 hr, and was ± 1.4 percent for the low power flow rates thereafter. As the figure shows, the total PMS flow rate was typically within 0.8 percent of that measured by the main mass flow controller during full power operation. However, this percentage difference increased during low power operation to 0.8 to 1.7 percent. This increased difference at the lower flow rates was largely due to a poor main LPA branch flow calibration, which dominated the total flow rate and tended to yield larger errors at lower flow rates (Ref. 27).

The PMS-indicated mass flow rates for all three LPA branches as a function of time are plotted in Figure 26. These flow rates showed that all three branch flow rates were steady, with the main flow regulated within a 0.2 sccm bandwidth, and the cathode and neutralizer flow rates regulated to a < 0.05 sccm bandwidth. The LPA proportional flow control valve pressure regulation design regulated LPA branch pressures to within ± 270 Pa (± 0.04 psi) throughout the wear test, as measured by the LPA branches' pressure transducers. Such a pressure variation would result in a worst case flow rate variation of ± 0.6 percent of flow setting. Cathode and neutralizer thermal throttle temperatures were steady to within ± 0.1 °C throughout the wear test, which would have resulted in a worst case flow variation of only ± 0.05 percent. Main thermal throttle temperatures were steady to within $+0.7/-0.5$ °C throughout the wear test, which would have resulted in a worst case flow variation of ± 0.2 percent. The slightly larger temperature variation of the main thermal throttle was likely due to a poor tuning of the proportional-integral-derivative loop tuning, which was made of commercially available hardware (Ref. 27).

The HPA proportional flow control valve pressure regulation design regulated the HPA outlet pressure to within ± 210 Pa (± 0.03 psi). The HPA outlet pressure was independently measured with a separate pressure transducer, labeled Pi in Figure 5. The discrepancy between the two pressure transducers was always within 2.1 kPa (0.3 psia), which is within the uncertainty of the pressure transducers. These measurements were yet another independent verification of the PMS pressure regulation design approach.

Propellant management system power consumption during steady state operation is plotted as a function of wear test time on Figure 27. Because pressure transducer power was not monitored during the test, average measured pressure transducer powers were used from Reference 27. Total PMS power consumption was within 8.5 to 10.2 W throughout the wear test during steady state operation. The thermal throttles consumed 42 to 46 percent of the total power, while the proportional flow control valves

consumed 28 to 31 percent and the pressure transducers consumed 26 to 27 percent. Total PMS power consumption throughout the wear test was lower than the project-required maximum of 20 W.

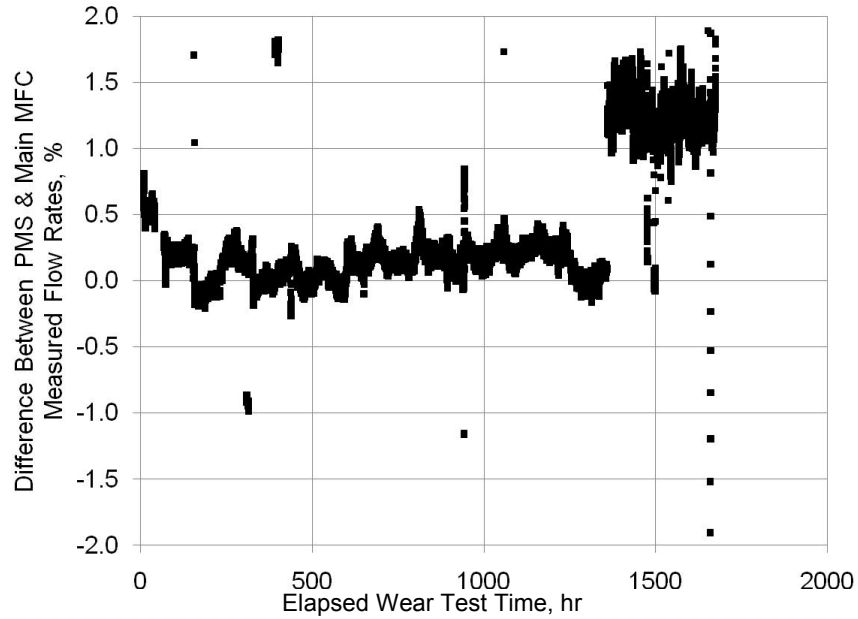


Figure 25.—Percentage difference between the total PMS flow rate and the main mass flow meter measurement as a function of wear test time.

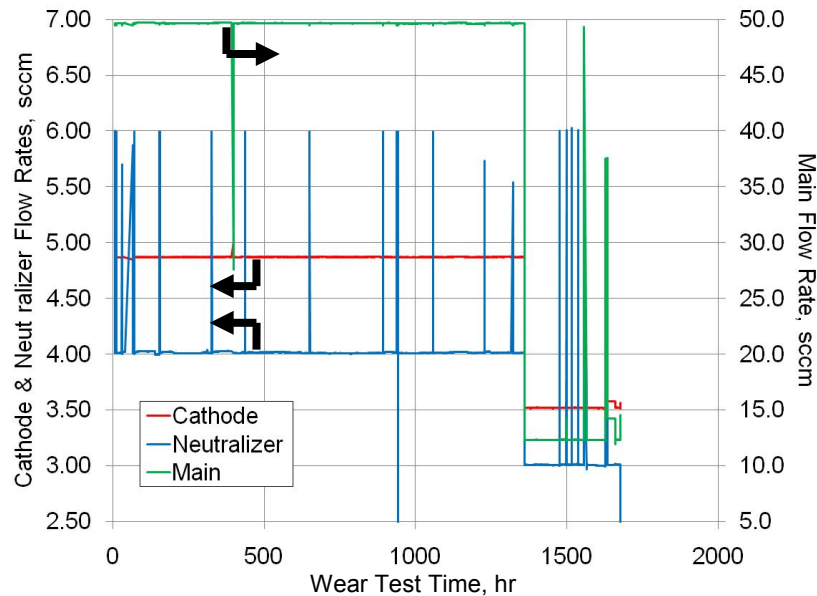


Figure 26.—Mass flow rates measured by the PMS during the wear test. All flow spikes were due to wear test restarts or test interruptions.

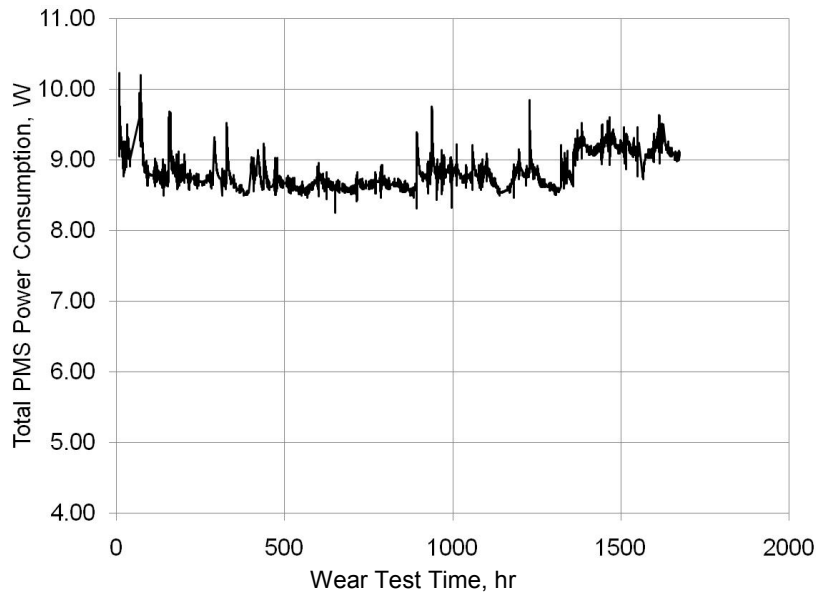


Figure 27.—Total PMS power consumption as a function of wear test time. Pressure transducer power was taken from Reference 27.

The calibration of each LPA branch was checked prior to and following the wear test. These calibration checks were conducted using the mass flow controllers of the XFSE, shown in Figure 5. The calibration process is described in greater detail in Reference 27. A comparison of the pre- and post-test calibration checks showed < 0.5 percent change for the main flow branch. For the cathode and neutralizer branches, calibration check results typically showed a 0.8 to 2 percent shift. It is difficult to conclude that this shift real, though, since the uncertainty in the mass flow controller used for the calibration check was 1.0 to 1.8 percent. Regardless, the calibration check results showed that LPA branch flow rates were within the branch flow rate requirement of ± 3 percent of the commanded flow.

Ion Engine Inspection Results

After the wear-test, thruster PM1R was partially disassembled such that inspections could be made of the ion optics, Discharge Cathode Assembly (DCA), Neutralizer Cathode Assembly (NCA), interior wiring, and the internal propellant feed system. The thruster in various states of assembly is shown in Figure 28. Inspection results of the major thruster subassemblies follow.

Discharge Chamber

The discharge chamber surfaces, as shown in Figure 28, are discolored but are in excellent condition. The chamber wire mesh, which was grit blasted to ensure coatings were retained, showed no evidence of spalling. Some debris was found in the chamber. Almost all the debris had dimensions < 0.5 mm, and much of it was on the mesh covering the magnet rings. Most of the debris was found on the cylindrical magnet ring. Results of X-ray Energy Dispersive Spectroscopy indicated the debris was comprised primarily of iron, chromium, nickel, and carbon. Since there is no stainless steel in the discharge chamber internal parts that are susceptible to sputtering, the source of the debris is likely from the vacuum facility. The ion optics' apertures are much larger than the debris dimensions. Thus the ion optics provided access for the debris to enter the discharge chamber either during the venting of the vacuum chamber or during removal of hardware from the vacuum chamber.

The magnetic fields were measured at the DCA keeper orifice plate and at the surface of the magnet rings. Given the accuracy of the measurements, there was no change in values of the magnetic fields from

the initial thruster assembly to the end of testing, which included the performance acceptance tests, vibration tests, thermal vacuum tests, and the wear test.

Discharge Cathode Assembly

The DCA includes the hollow cathode, cathode heater, and a keeper electrode that is made of graphite, which ensures that most of the cathode orifice plate is protected from ion bombardment. A photograph of the keeper and cathode orifice plates is shown in Figure 29. As shown in the figure, there is no evidence of chamfering of the orifice plates due to ion erosion. Changes in keeper and cathode orifice diameters were within the measurement accuracy of 0.025 mm. The keeper to cathode electrode gap was within the required specifications. High voltage impedance measurements between the keeper and the cathode indicated no evidence of flakes bridging the electrode gap immediately after the wear test or during the various segments of the inspection process. No life limiting issues relative to the DCA were found during the wear test or post test inspections.

Neutralizer Cathode Assembly

The NCA is comprised of the hollow cathode, the cathode heater, and the keeper electrode. Visual and photographic inspection indicated the NCA was in good condition after the wear test. Both orifice plates showed discolorations over their surfaces. Figure 30 shows that there is some slight evidence of these discolorations before and after the wear test. The cathode orifice plate has some ion texturing of the surface, particularly in the chamfer region.



Figure 28.—Thruster PM1R in various states of assembly following the wear test.



Figure 29.—Discharge cathode and keeper orifice following the wear test.

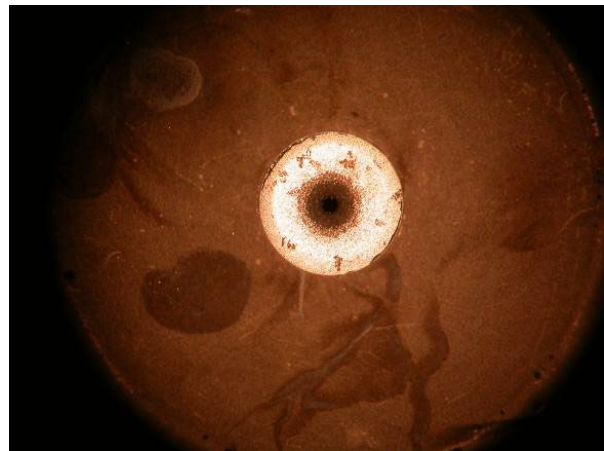


Figure 30.—Neutralizer cathode and keeper orifice plate following the wear test.

The change in keeper and cathode orifice diameters over the course of the test was within the measurement uncertainty of 0.025 mm. The electrode gap was measured post test and was found to be within specifications. High voltage impedance checks immediately after the wear test and during the inspection phase indicated no evidence of flakes bridging the cathode-keeper gap.

The keeper tube is exposed to erosion from wide-angle beam ions. Measurements of the keeper tube diameter from the orifice plate to 28 mm upstream of it indicated there was no change in keeper diameter within the measurement accuracy. Erosion of the neutralizer keeper tube by primary ions over the life of the neutralizer was undetectable.

Ion Optics

Pin gages were used to measure the aperture diameters of the screen grid and the accelerator grid. From the initial assembly of the thruster to the post test inspection there was no measured change in the pin gauge measurements within the accuracy of the measurements. Changes in gap are also within the accuracy of the measurements. This is consistent with the ion optics of the LDT where the cold grid gap at the center has been not been changing (Ref. 20). This finding is further evidence that the problem of the changing grid gap in the NSTAR design has been resolved. The lack of changes in the grid gap and the aperture diameter also supports the observation that there has been negligible change in electron backstreaming. Figures 31, 32, and 33 show the accelerator grid center aperture after the initial 2000-hr test of EM1 (Ref. 19), the LDT after 2176 hr (Ref. 35), and after the PM1R thruster test with 2098 hr of testing, respectively. The 2000-hr test grid clearly shows evidence of the usual pit and groove erosion from charge exchange ions. The image from the LDT does not clearly show evidence of pit erosion at the hexagon vertices. The image from the subject wear test shows accelerator grid groove erosion, but there is very little evidence of pits. Laser profilometry measurements of the center aperture are shown in Figure 34. These measurements indicate a groove depth of 3.1 percent of the accelerator thickness and a pit depth of 5.6 percent of the accelerator thickness. Figure 35 shows the accelerator grid outer radius apertures, which are distorted by “erosion ears.” The aperture “ears” are expected (Refs. 35 and 36). Erosion of the “ears” is complete after a few hundred hours, and this effect should not compromise performance or grid lifetime. The basic observations of the ion optics’ dimensions and erosion patterns do not differ significantly from the results of the ongoing NEXT LDT that has operated for over 24,400 hr (Refs. 20 and 21).

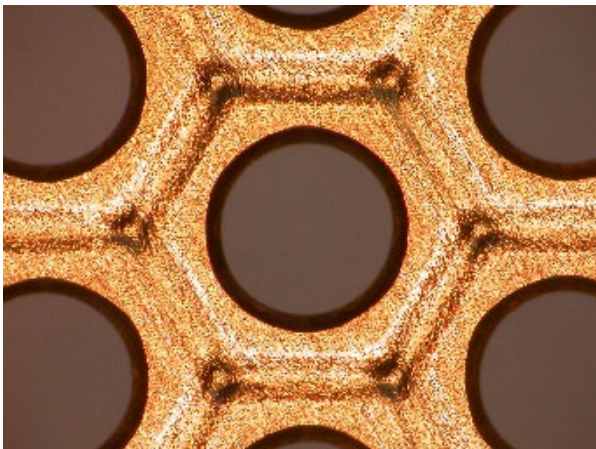


Figure 31.—Thruster EM1 accelerator center aperture after 2000 hr test.

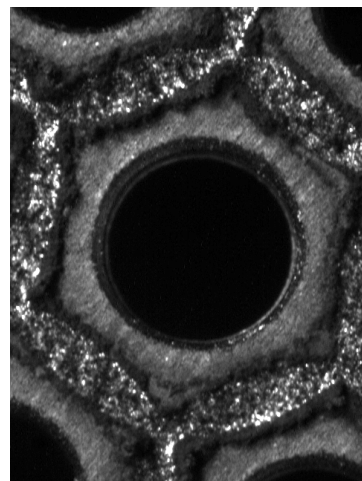


Figure 32.—Thruster EM3 accelerator center aperture at 2176 hr in LDT.

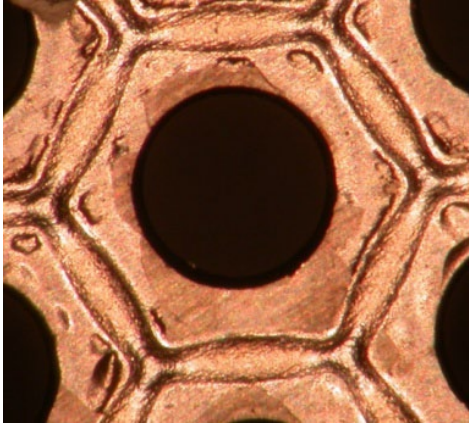


Figure 33.—Thruster PM1R accelerator center aperture after 2098 hr.

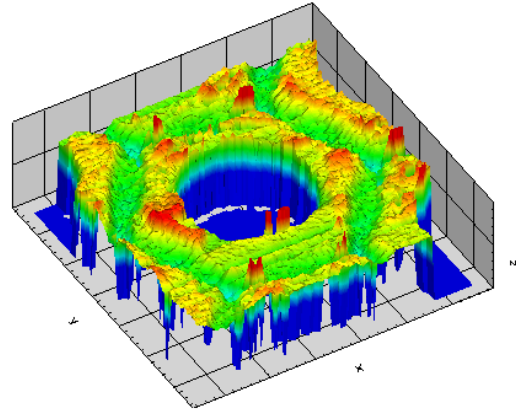


Figure 34.—Profilometry image of PM1R center aperture after the wear test.



Figure 35.—Thruster PM1R accelerator grid outer apertures after the wear test.

Ion Engine Service Life Assessment

The PM1R wear test results are consistent with the service life assessment of the NEXT thruster (Refs. 15 and 16). These results are also consistent with the ongoing LDT using an EM engine and PM optics (Ref. 20). The primary life limiter of the NEXT thruster is still expected to be the structural failure of the accelerator grid when the groove penetrates the accelerator grid. The model described in References 15 and 16 predicted that, based on throttling shown in Table 3, the groove depth would be 5.0 percent of the accelerator thickness. The PM1R optics show 3.1 percent groove penetration after 2098 hr of operation on the optics, of which 1436 hr is at full power. Part of the difference between the model and the test results is from the effect of the backspattered material on the optics. Still, the PM1R wear test results indicate that the lifetime model used yields conservative lifetime predictions. The hardware and performance observations from the PM1R wear test indicate that PM thruster lifetimes should be comparable to the EM version thrusters, particularly EM3 in the LDT which has optics of the PM design.

Conclusion

The results of the NEXT PM1R wear test were presented. The NEXT PM1R thruster and PMS successfully demonstrated extended operation for 1618 hr with beam extraction during the wear test, corresponding to 30.5 kg of xenon processed, before voluntary termination. During the wear test, the thruster operated for 1312 hr at full power, 277 hr at low power, and the remainder of the time at intermediate power points for performance testing. The thruster performance is characterized over the throttling range of 0.5 to 6.9 kW, with calculated thrust of 26 to 237 mN, respectively. Overall thruster performance, which includes thrust, input power, specific impulse, and thrust efficiency, has remained constant with negligible signs of degradation. Perveance margins and electron backstreaming margins have also shown no decrease. While the discharge current has increased ~ 0.7 A during the test at full power, the discharge losses have increased by at most 1 to 2 W/A. Generally, the discharge losses have varied by 4 W/A, which is slightly larger than the 2 W/A exhibited during the LDT and is suspected to be from a change in thermal losses in the cathode. Although a leak was found after the wear test, the neutralizer transition flow margin has decreased 0.3 sccm over the duration of the test, similar to the NEXT thruster in the LDT. The grid gap and the accelerator aperture diameters have not changed within the accuracy of the measurement from beginning of life to the end of the wear test. This shows the same behavior as the optics in the LDT and indicates that the NEXT PM design will not suffer the problems associated with a changing grid gap that the NSTAR thruster experienced, such as a reduction in electron backstreaming margin. The PM1R groove erosion is 3.1 percent of the grid thickness for 2098 hr of operation, of which 1436 hr is at full power.

The PMS performed without incident during the wear test. The total PMS flow rate was typically within 0.8 percent of that measured by the main mass flow controller of the XFSE during full power operation. This percentage difference increased during low power operation to 0.8 to 1.7 percent. Flow rates from all three branches were steady, with the main flow regulated within a 0.2 sccm bandwidth, and the cathode and neutralizer flow rates regulated to a < 0.05 sccm bandwidth. Total PMS power consumption was within 8.5 to 10.2 W throughout the wear test during steady state operation. This power was substantially lower than the project-required maximum of 20 W. Calibration check results showed that LPA branch flow rates were within the branch flow rate requirement of ± 3 percent of the commanded flow.

The trends in performance and observation of the PM1R hardware post-test support that the EM hardware used in the LDT is representative of the expected changes throughout the life of the PM thrusters. The results of this test are also consistent with NEXT thruster life assessments to date.

References

1. Benson, S.W., Patterson, M.J., Vaughan, D.A., Wilson, A.C., and Wong, B.R., "NASA's Evolutionary Thruster (NEXT) Phase 2 Developmental Status," 41st Joint Propulsion Conference and Exhibit, AIAA-2005-4070, Tucson, AZ, Jul. 2005.
2. Patterson, M.J. and Benson, S.W., "NEXT Ion Propulsion System Development Status and Performance," 43rd Joint Propulsion Conference and Exhibit, AIAA-2007-5199, Cincinnati, OH, Jul. 2007.
3. Mankins, J.C., "Technology Readiness Levels," White Paper, Apr. 5, URL: <http://www.hq.nasa.gov/office/codeq/trl/trl.pdf> [cited 5 June, 2007].
4. Oh, D., Benson, S., Witzberger, K., and Cupples, M., "Deep Space Mission Applications for NEXT: NASA's Evolutionary Xenon Thruster," 40th Joint Propulsion Conference and Exhibit, AIAA-2004-3806, Fort Lauderdale, FL, Jul. 2004.
5. Sengupta, A., et al., "An Overview of the Results from the 30,000 Hr Life Test of Deep Space 1 Flight Spare Ion Engine," 40th Joint Propulsion Conference and Exhibit, AIAA-2004-3608, Fort Lauderdale, FL, Jul. 2004.

6. Polk, J.E., Anderson, J.R., Brophy, J.R., Rawlin, V.K., Patterson, M.J., Sovey, J., and Hamley, J., "An Overview of the Result from the 8200 Hour Wear Test of the NSTAR Ion Thruster," 35th Joint Propulsion Conference and Exhibit, AIAA-1999-2446, Los Angeles, CA, Jun. 1999.
7. Patterson, M. J., Rawlin, V. K., Sovey, J. S., Kussmaul, M. J., and Parkes, J., "2.3 kW Ion Thruster Wear Test," 31st Joint Propulsion Conference and Exhibit, AIAA-95-2516, San Diego, CA, Jul. 1995.
8. Polk, J.E., et al., "A 1000-Hour Wear Test of the NASA NSTAR Ion Thruster," 32nd Joint Propulsion Conference and Exhibit, AIAA-1996-2717, Lake Buena Vista, FL, Jul. 1996.
9. Brophy, J.R., Polk, J.E., and Rawlin, V.K., "Ion Engine Service Life Validation by Analysis and Testing," 32nd Joint Propulsion Conference and Exhibit, AIAA-1996-2715, Lake Buena Vista, FL, Jul. 1996.
10. Patterson, M.J., et al., "NEXT: NASA's Evolutionary Xenon Thruster Development Status," 39th Joint Propulsion Conference and Exhibit, AIAA-2003-4862, Huntsville, AL, Jul. 2003.
11. Emhoff, J.W. and Boyd, I.D., "Progress in NEXT Ion Optics Modeling," 40th Joint Propulsion Conference and Exhibit, AIAA-2004-3786, Fort Lauderdale, FL, Jul. 2004.
12. Farnell, C.C. and Williams, J.D., and Wilbur, P.J., "NEXT Ion Optics Simulation Via ffx," 39th Joint Propulsion Conference and Exhibit, AIAA-2003-4869, Huntsville, AL, Jul. 2003.
13. Emhoff, J.W. and Boyd, I.D., "Grid Erosion Modeling of the NEXT Ion Thruster Optics," 39th Joint Propulsion Conference and Exhibit, AIAA-2003-4868, Huntsville, AL, Jul. 2003.
14. Kovaleski, S.D., "Life Model of Hollow Cathode using a Barium Calcium Aluminate Impregnated Tungsten Emitter," 27th International Electric Propulsion Conference, IEPC-01-276, Pasadena, CA, Oct. 2001.
15. Van Noord, J.L. and Herman, D.A., "Application of the NEXT Ion Thruster Lifetime Assessment to Thruster Throttling," 44th ASEE Joint Propulsion Conference & Exhibit, AIAA-2008-4526, Hartford, CT, Jul. 2008.
16. Van Noord, J.L., "Lifetime Assessment of the NEXT Ion Thruster," 43rd Joint Propulsion Conference and Exhibit, AIAA-2007-5274, Cincinnati, OH, Jul. 2007.
17. Herman, D.A., Patterson, M.J., and Soulas, G.S., "NEXT Long-Duration Test Plume and Wear Characteristics after 17,200 h of Operation and 352 kg of Xenon Processed," 44th ASEE Joint Propulsion Conference & Exhibit, AIAA-2008-4919, Hartford, CT, Jul. 2008.
18. Herman, D.A., Patterson, M.J., and Soulas, G.S., "Performance Characteristics of the NEXT Long-Duration Test after 17,200 h of Operation and 352 kg of Xenon Processed," 44th Joint Propulsion Conference & Exhibit, AIAA-2008-4527, Hartford, CT, Jul. 2008.
19. Soulas, G.C., Kamhawi, H., Patterson, M.J., Britton, M. A., and Frandina, M.M., "NEXT Ion Engine 2000 Hour Wear Test Results," 40th Joint Propulsion Conference and Exhibit, AIAA-2004-3791, Fort Lauderdale, FL, Jul. 2004.
20. Herman, D.A., Soulas, G.C., and Patterson, M.J., "Status of the Long-Duration Test after 23,300 Hours of Operation," 45th Joint Propulsion Conference and Exhibit, AIAA-2009-4917, Denver, CO, Aug. 2009.
21. Herman, D.A., Soulas, G.C., and Patterson, M.J., "NEXT Long-Duration Test Neutralizer Performance and Erosion Characteristics," 31st International Electric Propulsion Conference, IEPC-2009-154, Ann Arbor, MI, Sep. 2009.
22. Soulas, G.C., Domonkos, M.T., and Patterson, M.J., "Performance Evaluation of the NEXT Ion Engine," 39th Joint Propulsion Conference and Exhibit, AIAA Paper 5278, Huntsville, AL, Jul. 2003.
23. Hoskins, W.A., et al., "Development of a Prototype Model Ion Thruster for the NEXT System," 40th Joint Propulsion Conference and Exhibit, AIAA-2004-4111, Fort Lauderdale, FL, Jul. 2004.
24. Herman, D.A., Soulas, G.C., and Patterson, M.J., "Performance Evaluation of the Prototype-model NEXT Ion Thruster," 43rd Joint Propulsion Conference and Exhibit, AIAA-2007-5212, Cincinnati, OH, Jul. 2007.
25. Snyder, J.S., et al., "Environmental Testing of the NEXT PM1 Ion Engine," 43rd Joint Propulsion Conference and Exhibit, AIAA-2007-5275, Cincinnati, OH, Jul. 2007.

26. Snyder, J.S., et al., "Environmental Testing of the NEXT PM1R Ion Engine," 30th International Electric Propulsion Conference, IEPC-2007-276, Florence, Italy, Sept. 2007.
27. Soulas, G.C., et al., "NEXT Single String Integration Test Results," 45th Joint Propulsion Conference and Exhibit, AIAA-2009-4816, Denver, CO, Aug. 2009.
28. Aadland, et al., "Development Results of the NEXT Propellant Management System," JANNAF Proceedings, Dec. 2005.
29. Aadland, R.S. and Talerico, L., "NEXT Propellant Management System (PMS) Thermal Vacuum Cycle Test Report," Aerojet Internal Report 2007-R-2948, Aug. 2007.
30. Pinero, L.R., et al., "Power Console Development for NASA's Electric Propulsion Outreach Program," International Electric Propulsion Conference, IEPC-93-250, Seattle, WA, Sep. 1993.
31. Soulas, G.C. and Patterson, M.J., "NEXT Ion Thruster Performance Dispersion Analyses," 43rd Joint Propulsion Conference and Exhibit, AIAA Paper 2007-5213, Cincinnati, OH, Jul. 2007.
32. Frandina, M.M., Arrington, L.A., Soulas, G.C., Hickman, T.A., and Patterson, M.J., "Status of the NEXT Ion Thruster Long Duration Test," 41st Joint Propulsion Conference and Exhibit, AIAA-2005-4065, Tucson, AZ, Jul. 2005.
33. Anderson, J.R., et al., "Results of On-going Long Duration Ground Test of the DS1 Flight Spare Ion Engine," 35th Joint Propulsion Conference and Exhibit, AIAA-99-2857, Los Angeles, CA, June 1999.
34. Soulas, G.C., "Performance of Titanium Optics on a NASA 30 cm Ion Thruster," 36th AIAA joint Propulsion Conference, Huntsville, AL, AIAA-2000-3814, Jul. 2000.
35. Herman, D.A., Soulas, G.C., and Patterson, M.J., "Status of the NEXT Ion Thruster Long-Duration Test after 10,100 h and 207 kg Demonstrated," 43rd Joint Propulsion Conference and Exhibit, AIAA-2007-5272, Cincinnati, OH, Jul. 2007.
36. Malone, S.P., "Investigation of NEXT Ion Optics Erosion Processes Using Computational Modeling," 52nd Joint Army-Navy-NASA-Air Force (JANNAF) Propulsion Meeting (JPM), Monterey, CA, Dec. 2005.

REPORT DOCUMENTATION PAGE			Form Approved OMB No. 0704-0188		
<p>The public reporting burden for this collection of information is estimated to average 1 hour per response, including the time for reviewing instructions, searching existing data sources, gathering and maintaining the data needed, and completing and reviewing the collection of information. Send comments regarding this burden estimate or any other aspect of this collection of information, including suggestions for reducing this burden, to Department of Defense, Washington Headquarters Services, Directorate for Information Operations and Reports (0704-0188), 1215 Jefferson Davis Highway, Suite 1204, Arlington, VA 22202-4302. Respondents should be aware that notwithstanding any other provision of law, no person shall be subject to any penalty for failing to comply with a collection of information if it does not display a currently valid OMB control number.</p> <p>PLEASE DO NOT RETURN YOUR FORM TO THE ABOVE ADDRESS.</p>					
1. REPORT DATE (DD-MM-YYYY) 01-11-2010		2. REPORT TYPE Technical Memorandum		3. DATES COVERED (From - To)	
4. TITLE AND SUBTITLE NASA's Evolutionary Xenon Thruster (NEXT) Prototype Model 1R (PM1R) Ion Thruster and Propellant Management System Wear Test Results			5a. CONTRACT NUMBER		
			5b. GRANT NUMBER		
			5c. PROGRAM ELEMENT NUMBER		
6. AUTHOR(S) Van Noord, Jonathan, L.; Soulas, George, C.; Sovey, James, S.			5d. PROJECT NUMBER		
			5e. TASK NUMBER		
			5f. WORK UNIT NUMBER WBS 346620.04.05.03.11		
7. PERFORMING ORGANIZATION NAME(S) AND ADDRESS(ES) National Aeronautics and Space Administration John H. Glenn Research Center at Lewis Field Cleveland, Ohio 44135-3191			8. PERFORMING ORGANIZATION REPORT NUMBER E-17492		
9. SPONSORING/MONITORING AGENCY NAME(S) AND ADDRESS(ES) National Aeronautics and Space Administration Washington, DC 20546-0001			10. SPONSORING/MONITOR'S ACRONYM(S) NASA		
			11. SPONSORING/MONITORING REPORT NUMBER NASA/TM-2010-216916		
12. DISTRIBUTION/AVAILABILITY STATEMENT Unclassified-Unlimited Subject Category: 20 Available electronically at http://gltrs.grc.nasa.gov This publication is available from the NASA Center for AeroSpace Information, 443-757-5802					
13. SUPPLEMENTARY NOTES					
14. ABSTRACT The results of the NEXT wear test are presented. This test was conducted with a 36-cm ion engine (designated PM1R) and an engineering model propellant management system. The thruster operated with beam extraction for a total of 1680 hr and processed 30.5 kg of xenon during the wear test, which included performance testing and some operation with an engineering model power processing unit. A total of 1312 hr was accumulated at full power, 277 hr at low power, and the remainder was at intermediate throttle levels. Overall ion engine performance, which includes thrust, thruster input power, specific impulse, and thrust efficiency, was steady with no indications of performance degradation. The propellant management system performed without incident during the wear test. The ion engine and propellant management system were also inspected following the test with no indication of anomalous hardware degradation from operation.					
15. SUBJECT TERMS Ion thruster; Ion optics; Hollow cathodes; Electric propulsion; Electrostatic propulsion					
16. SECURITY CLASSIFICATION OF:			17. LIMITATION OF ABSTRACT UU	18. NUMBER OF PAGES 35	19a. NAME OF RESPONSIBLE PERSON STI Help Desk (email:help@sti.nasa.gov)
a. REPORT U	b. ABSTRACT U	c. THIS PAGE U			19b. TELEPHONE NUMBER (include area code) 443-757-5802

